



HAL
open science

Cell-specific pathways recruited for symbiotic nodulation in the *Medicago truncatula* legume

Sergio Alan Cervantes-Pérez, Sandra Thibivilliers, Carole Laffont, Andrew Farmer, Florian Frugier, Marc Libault

► To cite this version:

Sergio Alan Cervantes-Pérez, Sandra Thibivilliers, Carole Laffont, Andrew Farmer, Florian Frugier, et al.. Cell-specific pathways recruited for symbiotic nodulation in the *Medicago truncatula* legume. *Molecular Plant*, In press, 10.1016/j.molp.2022.10.021 . hal-03867628

HAL Id: hal-03867628

<https://hal.science/hal-03867628>

Submitted on 23 Nov 2022

HAL is a multi-disciplinary open access archive for the deposit and dissemination of scientific research documents, whether they are published or not. The documents may come from teaching and research institutions in France or abroad, or from public or private research centers.

L'archive ouverte pluridisciplinaire **HAL**, est destinée au dépôt et à la diffusion de documents scientifiques de niveau recherche, publiés ou non, émanant des établissements d'enseignement et de recherche français ou étrangers, des laboratoires publics ou privés.

Journal Pre-proof

Cell-specific pathways recruited for symbiotic nodulation in the *Medicago truncatula* legume

Sergio Alan Cervantes-Pérez, Sandra Thibivilliers, Carole Laffont, Andrew D. Farmer, Florian Frugier, Marc Libault

PII: S1674-2052(22)00373-2

DOI: <https://doi.org/10.1016/j.molp.2022.10.021>

Reference: MOLP 1454

To appear in: *MOLECULAR PLANT*

Received Date: 10 August 2022

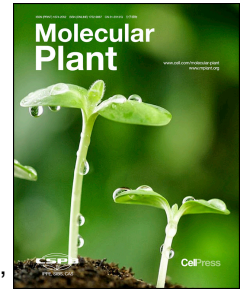
Revised Date: 5 October 2022

Accepted Date: 27 October 2022

Please cite this article as: Cervantes-Pérez S.A., Thibivilliers S., Laffont C., Farmer A.D., Frugier F., and Libault M. (2022). Cell-specific pathways recruited for symbiotic nodulation in the *Medicago truncatula* legume. Mol. Plant. doi: <https://doi.org/10.1016/j.molp.2022.10.021>.

This is a PDF file of an article that has undergone enhancements after acceptance, such as the addition of a cover page and metadata, and formatting for readability, but it is not yet the definitive version of record. This version will undergo additional copyediting, typesetting and review before it is published in its final form, but we are providing this version to give early visibility of the article. Please note that, during the production process, errors may be discovered which could affect the content, and all legal disclaimers that apply to the journal pertain.

© 2022 The Author



1 **Cell-specific pathways recruited for symbiotic nodulation in the *Medicago truncatula* legume**
2 Sergio Alan Cervantes-Pérez^{1#}, Sandra Thibivilliers^{1,2#}, Carole Laffont³, Andrew D. Farmer⁴,
3 Florian Frugier³, Marc Libault^{1,2,*}

4

5 ¹ Department of Agronomy and Horticulture, Center for Plant Science Innovation, University of
6 Nebraska-Lincoln, Lincoln, NE, 68503, USA

7 ² Single Cell Genomics Core Facility; Center for Biotechnology, University of Nebraska-Lincoln,
8 NE 68588, USA.

9 ³ Institute of Plant Sciences Paris-Saclay (IPS2), Université Paris-Saclay, CNRS, INRAE,
10 Université Paris-Cité, Université d'Evry, Gif-sur-Yvette, 91190, France

11 ⁴ National Center for Genome Resources, Santa Fe, NM, 87505, USA

12 # Contributed equally

13

14 Contact: marc.libault@unl.edu

15

16 **Running Title:** Medicago single-cell RNA-seq response to rhizobia

17

18 **Short Summary:** Legume nodulation is the result of the symbiotic interaction between legume
19 plants and soil bacteria collectively named rhizobia. In this study, upon applying single-nucleus
20 RNA-seq technology, we generated a single-cell resolution transcriptomic map of the Medicago
21 root. Using this map, we conducted a comprehensive transcriptomic analysis of the early root
22 symbiotic responses at a cell-type-specific level.

23

24

25

26

27

28

29

30

31

Abstract

Medicago truncatula is a model legume species that has been studied for decades to understand the symbiotic relationship between legumes and soil bacteria collectively named rhizobia. This symbiosis called nodulation is initiated in roots with the infection of root hair cells by the bacteria as well as the initiation of nodule primordia from root cortical, endodermal, and pericycle cells, leading to the development of a new root organ, the nodule, where bacteria fix and assimilate the atmospheric dinitrogen for the benefit of the plant. Here, we report the isolation and use of nuclei from mock and rhizobia-inoculated roots to conduct single nuclei RNA-seq (sNucRNA-seq) experiments to gain a deeper understanding of early responses to rhizobial infection in *Medicago* roots. A gene expression map of the *Medicago* root was generated, comprising 25 clusters, which were annotated as specific cell-types using 119 *Medicago* marker genes and orthologs to *Arabidopsis* cell-type marker genes. A focus on root hair, cortex, endodermis, and pericycle cell-types, showing the strongest differential regulations in response to a short-term (48 hours) rhizobium inoculation, revealed both known genes and functional pathways, validating the sNucRNA-seq approach, but also numerous novel genes and pathways, allowing a comprehensive analysis of early root symbiotic responses at a cell-type-specific level.

Keywords: *Medicago* root, single-cell transcriptomic, rhizobium, nodule initiation, root hair cells, cortical cells

51
52
53
54
55
56
57
58
59
60
61
62

63 Introduction

64 Legumes symbiotically interact with nitrogen-fixing soil bacteria collectively named
65 rhizobia. The molecular, physiological, and cellular responses of this symbiosis named nodulation
66 have been extensively studied over the past decades (Roy et al., 2019). Legume nodulation is a
67 complex biological process that requires the activation of temporally and spatially coordinated
68 programs in a limited number of root cells. Briefly, legume nodulation is initiated by the perception
69 of the rhizobial lipochitooligosaccharide Nod factors (NFs) and the subsequent infection of plant
70 root hair cells by rhizobia. Concomitantly, a nodule primordium emerges. In *Medicago truncatula*,
71 a legume species generating indeterminate nodules, these primordia are initiated from cell
72 divisions within the root inner cortex, endodermis, and pericycle layers, and an apical meristem is
73 then established and maintained during the entire life of the nodule. Rhizobia infect the developing
74 root nodule primordia, differentiate into bacteroids, and fix and assimilate the atmospheric
75 dinitrogen allowing a steady supply of nitrogen for the plant.

76 Functional genomic studies revealed the role of many legume genes controlling the early
77 stages of nodulation, notably in root hair cells (trichoblasts) where the initial microsymbiont
78 perception and the rhizobial infection take place, but also to a lower extent in pericycle and cortex
79 inner root cell layers where nodule organogenesis initiates (Roy *et al.*, 2019). Several *M.*
80 *truncatula* genes have been functionally characterized to control the infection of the root
81 epidermis. Among them, *MtNPL* [Nodule Pectate Lyase; (Xie et al., 2012)], a gene encoding a cell
82 wall degrading enzyme required for the initiation of infection threads in curled root hairs, *MtLIN*
83 [Lumpy Infections; (Kiss et al., 2009; Liu et al., 2019a)], which encodes a putative E3 ligase,
84 *MtRPG* [Rhizobium Directed Polar Growth; (Arrighi et al., 2008)], a gene encoding a protein with
85 a coiled-coiled domain, *MtFLOT4* (Haney and Long, 2010), *MtVPPY* (Murray et al., 2011),
86 NADPH oxidase/respiratory burst oxidase homologs [e.g., Rboh; (Montiel et al., 2016)], and
87 *MtCBSI*, a gene encoding a Cystathionine- β -Synthase-like Domain-Containing Protein (Sinharoy
88 et al., 2016), are all upregulated in response to rhizobium inoculation. In addition, other rhizobium-
89 upregulated genes participate in the NF signaling pathway such as LYsM receptors that perceive
90 NF bacterial signals. These genes belong to the LysM receptor kinase and LYK-related gene
91 families [*MtLYK* and *MtLYR*, respectively; e.g. *MtNFP* (NF Perception; (Gough et al., 2018))],
92 *MtDMII*, 2 and 3 (Does not Make Infections) genes (Ané et al., 2004; Endre et al., 2002; Gleason
93 et al., 2006), *MtPUB1* and 2 (Plant U-box protein 1 and 2) involved in protein degradation (Liu et

94 al., 2018; Mbengue et al., 2010), *MtNFHI* [NF Hydrolase 1; (Cai et al., 2018)] that controls NF
95 degradation, *MtIPD3* [Interacting with DMI3; (Messinese et al., 2007)], and various transcription
96 factor (TF) genes [e.g., *MtNSPI/2* (Nodulation Signaling Pathway 1/2; (Kaló et al., 2005; Smit et
97 al., 2005)), *MtNF-YA1* (Nuclear factor-YA1; (Combier et al., 2006)), *MtERN1* (ERF (Ethylene
98 Response Factor) Required for Nodulation; (Andriankaja et al., 2007; Middleton et al., 2007)), and
99 *MtNIN* (Nodule Inception; (Schauser et al., 1999))].

100 To date, a limited number of studies have highlighted the regulatory mechanisms
101 controlling the response of inner root cell layers to rhizobial inoculation (i.e., pericycle,
102 endodermis, and cortex). Among them, cytokinin signaling is necessary and sufficient to promote
103 the initiation of nodule primordia and inhibit the response of epidermal root cells to rhizobia and
104 NFs (Boivin et al., 2016; Gamas et al., 2017; Gonzalez-Rizzo et al., 2006; Jardinaud et al., 2016;
105 Lin et al., 2021; Murray et al., 2007; Plet et al., 2011). Genes controlling root development were
106 also shown to be recruited for nodule development, such as *MtPLT* [Plethora; (Franssen et al.,
107 2015)], *MtKNOX* [Knotted homeobox; (Di Giacomo et al., 2017)], *MtLBD16* [LOB Binding
108 Domain 16; (Schiessl et al., 2019; Soyano et al., 2019)], *MtSHR* [ShortRoot; (Dong et al., 2021)],
109 *MtSCR* [Scarecrow; (Dong et al., 2021)], and *MtNOOT1* (Shen et al., 2019). On some occasions,
110 genes were shown to have a dual function to promote root epidermal infection and nodule initiation
111 at the level of the pericycle and cortical cells, such as *MtNIN* (Liu et al., 2019b).

112 To gain a more accurate picture of the symbiotic transcriptional programs controlling the
113 root hair signal perception and infection, transcriptomic studies were conducted on populations of
114 isolated legume root hair cells using root hair shaving or laser dissection (Breakspear et al., 2014;
115 Libault et al., 2009). Similarly, -omics analyses targeting the zone of emerging nodules revealed
116 the transcriptomic programs controlling the initiation and development of nodule primordia
117 (Larrainzar et al., 2015; Lohar et al., 2005; Schiessl et al., 2019; van Zeijl et al., 2015). While
118 valuable, these approaches suffer from the cellular heterogeneity of the isolated root hair
119 populations [i.e., a mixture of unresponsive, responsive but uninfected, and infected root hair cells
120 (Bhuvanewari et al., 1981)], and from the cellular complexity of the root. For instance, as a
121 reflection of the cellular heterogeneity of the root hair population, it has been estimated that only
122 1-5 % of the root hair cells are infected by rhizobia (Nutman, 1959).

123 While these approaches increased the resolution of plant transcriptomic analyses, they have
124 been recently superseded by the emergence of single-cell (scRNA-seq) and single-nucleus

125 (sNucRNA-seq) transcriptomic technologies. Here, we report the use of the sNucRNA-seq
126 technology on *M. truncatula* roots mock-inoculated or inoculated with its symbiont, *Ensifer*
127 (*Sinorhizobium*) *meliloti*, to precisely capture the transcriptomic programs induced during the early
128 stages of the nodulation process in each cell-type composing the *M. truncatula* root. The
129 establishment of a single-cell resolution transcriptomic map of the *M. truncatula* root allowed
130 characterizing the transcriptomic response of the *M. truncatula* root hair, cortical, endodermal, and
131 pericycle cells at an early stage (48 hours) after *E. meliloti* inoculation. The transcriptomic analysis
132 of these different cell-types revealed the dynamic regulation of *M. truncatula* genes in response to
133 rhizobial infection, including many novel genes and functional pathways, as well as the differential
134 recruitment of previously known nodulation-related and hormonal genes depending on cell-types.

135

136 **Results**

137 **Establishment of a transcriptional map of the rhizobium-inoculated *M. truncatula* root at a** 138 **single-cell level resolution**

139 Isolated plant protoplasts and nuclei have been successfully used to establish single-cell
140 resolution transcriptomes notably from Arabidopsis root cells (Denyer et al., 2019; Farmer et al.,
141 2021; Jean-Baptiste et al., 2019; Ryu et al., 2019; Shulse et al., 2019; Zhang et al., 2019). The high
142 correlation between cellular, nuclear, and whole root transcriptomes (Farmer *et al.*, 2021) supports
143 the biological relevance of both scRNA-seq and sNucRNA-seq approaches. However, the nuclear-
144 based transcriptomic technology has unique advantages compared to the protoplast-based
145 transcriptomic technology, including the ease of nuclei isolation from various plant species and
146 organs, and the limited induction of stress-related genes [i.e., in contrast, protoplastization leads
147 to the induction of hundreds of stress-responsive genes; (Birnbaum et al., 2003; Denyer *et al.*,
148 2019)]. Therefore, we conducted sNucRNA-seq experiments to characterize the transcriptomic
149 profiles of the different cell-types composing the Medicago root apex and their early response to
150 rhizobial inoculation.

151 Shortly, Medicago seedlings were inoculated 4 days post-germination with water or a
152 bacterial suspension of *E. meliloti* ($OD_{600nm}=0.1$). Forty-eight hours post-rhizobium inoculation,
153 root tips including fully elongated root hair cells were collected and committed to nuclei isolation
154 (see “Methods” for details). Three independent *E. meliloti*-inoculated and three independent mock-
155 inoculated sNucRNA-seq libraries were generated using the 10x Genomics Chromium platform.

156 To establish transcriptomic profiles of Medicago root cells, we applied a “pre-mRNA” strategy
157 using Cell Ranger (10x Genomics) to map sequencing reads against transcripts and introns of the
158 v1.8 annotation of the MtrunA17r5.0-ANR genome (Pecrix et al., 2018). This first step was
159 followed by the removal of the ambient transcriptomic noise and the detection and removal of
160 doublets (i.e., two nuclei encapsulated into the same reaction volume) (see Methods). To support
161 the quality of the libraries, we analyzed the distribution of the number of expressed genes per
162 nucleus and observed an expected normal distribution (Supplemental Figure 1). To remove outliers
163 and low-quality nuclei, we applied a 95% confidence interval to the normal distribution of the six
164 integrated libraries (Supplemental Figure 1). Taken together, the transcriptomes of 15,854 *E.*
165 *meliloti*-inoculated and 12,521 mock-inoculated *M. truncatula* root nuclei were further analyzed
166 (Supplemental Table 1), with a median value of 1,053 expressed genes per nucleus and a total of
167 31,307 expressed protein-coding genes detected [70.2% of the 44,615 Medicago protein-coding
168 genes (Pecrix *et al.*, 2018)]. Considering that the number of Arabidopsis and Medicago expressed
169 genes per nucleus are similar (i.e., 1,124 expressed genes per Arabidopsis nucleus), the percentage
170 of Medicago protein-coding genes expressed is less compared to Arabidopsis [i.e., 89.4% of
171 27,420 protein-coding genes (Farmer *et al.*, 2021)]. Such a limited percentage might be a
172 consequence of the neo- or sub-functionalization of Medicago genes following the whole-genome
173 duplication that occurred 58 million years ago, or the result of an over-estimation of the number
174 of protein-coding genes in Medicago compared to the reference Arabidopsis genome.

175 Using the Seurat package, we normalized and integrated 28,375 nuclei transcriptomes
176 before applying the uniform manifold approximation and projection (UMAP) technique to cluster
177 the nuclei according to their transcriptomic profiles. Twenty-five clusters were identified [Figure
178 1A; the dataset can be interrogated using the
179 [https://shinycell.legumeinfo.org/medtr.A17.gnm5.ann1_6.expr.Cervantes-
180 Perez_Thibivilliers_2022/](https://shinycell.legumeinfo.org/medtr.A17.gnm5.ann1_6.expr.Cervantes-Perez_Thibivilliers_2022/) web interface (Ouyang et al., 2021)], for which the percentage of nuclei
181 per cluster was not statistically different between inoculated and mock-inoculated conditions
182 (Student t-test > 0.05; Figure 1B; Supplemental Table 1). While *E. meliloti* inoculation did not
183 lead to changes in the number of clusters or the overall topography of the UMAP projection, we
184 repetitively noticed a local modification in the distribution of a subpopulation of cluster #2 nuclei
185 (Figure 1A, red circle). These results highlight that the *E. meliloti* inoculation induces significant
186 changes in the transcriptome of these Medicago root cells.

187

188 Functional annotation of Medicago root nuclei clusters

189 The functional annotation of root cells/nuclei according to their transcriptomic profile was
190 previously successfully achieved in the model species *A. thaliana* by exploring the transcriptional
191 pattern of a large number of functionally characterized cell-type-specific marker genes (Denyer *et al.*,
192 2019; Farmer *et al.*, 2021; Jean-Baptiste *et al.*, 2019; Ryu *et al.*, 2019; Shulse *et al.*, 2019;
193 Zhang *et al.*, 2019). To annotate the 25 nuclei clusters of the UMAP, we first analyzed the
194 transcriptional pattern of the few available functionally characterized Medicago root cell-type-
195 specific markers (Supplemental Table 2). The *MtPLT1-4* genes are specifically expressed in the
196 quiescent center of the root and nodule primordia (Franssen *et al.*, 2015). Looking at their
197 expression pattern in the Medicago UMAP, they are all preferentially expressed in the central star-
198 shaped cluster #9, supporting its annotation as the “stem cell niche” cluster (Figures 2A and B).
199 To annotate Medicago epidermal cells, the expression of the phosphate transporter *MtPT1* gene,
200 which is specifically expressed in Medicago root hairs and epidermal cells (Chiou *et al.*, 2001),
201 was analyzed. *MtPT1* was mostly expressed in clusters #1 and 2, and to a lesser extent, in cluster
202 #5 (Figure 2B). The root hair-specific *MtRbohF* gene (Marino *et al.*, 2011) was mostly expressed
203 in cluster #3 (Figure 2B), suggesting its annotation as “root hair cells”. To support the annotation
204 of the root epidermal cells, we also analyzed the expression of 45 genes previously identified as
205 specifically expressed in the root hair (Breakspear *et al.*, 2014) and 25 Medicago genes
206 orthologous to the 168 root-hair-specific Arabidopsis genes (Cvrčková *et al.*, 2010). Taken
207 together, most of these genes are preferentially or specifically expressed in the Medicago root
208 epidermal cells (Supplemental Figure 2, red rectangles), especially in cluster #3. Based on the
209 expression pattern of these different Medicago markers, clusters #1 and 2 could be thus confidently
210 annotated as “root epidermal cell” clusters, and cluster #3 as a “root hair cell” cluster (Figure 2A).
211 To identify the Medicago cortical cells on the UMAP projection, we analyzed the transcriptional
212 activity of the cortical cell-specific genes *MtIFS1*, *MtIFS3*, and *MtPAL5* (Biala *et al.*, 2017).
213 *MtIFS1* was almost specifically expressed, and *MtIFS3* and *MtPAL5* were preferentially expressed
214 in cluster #14 (Figure 2B). Besides, *MtIFS3* and *MtPAL5* are also detected in clusters #7 and 10,
215 and in clusters #18 and 19, respectively. Taken together, these results support the annotation of
216 cluster #14 as a “cortical cell” cluster. *MtSCR* is mostly expressed in the endodermis as well as in
217 cortical and epidermal cells (Dong *et al.*, 2021) and was thus used for annotating the endodermis

218 (Figure 2A). *MtSCR* was mostly detected in clusters #17, 18, and 19 that are co-localized on the
 219 UMAP projection (Figure 2B), which were thus annotated as “endodermal cell” clusters.
 220 *MtPHO1.1*, *MtPHO1.3*, and to a lesser extent, *MtPHO1.2*, are preferentially expressed in the root
 221 stele and more specifically in pericycle cells (Nguyen et al., 2020). *MtPHO1.1* and *MtPHO1.3*
 222 were most expressed in cluster #20, where *MtPHO1.2* is also highly expressed, as well as in cluster
 223 #5. The transcriptional activity of these three *PHO1* genes supports that cluster #20 is associated
 224 with the root pericycle and/or stele (Figure 2A). Other genes expressed in the root stele, such as
 225 *MtHext1/STP13*, *MtSHR1*, *MtSHR2*, and *MtPAL* (Biala et al., 2017; Dong et al., 2021; Gaude et
 226 al., 2012), were co-expressed in clusters #19 to 24 (Figure 2B). Considering that *MtSCR*, an
 227 endodermal cell marker gene, is highly expressed in cluster #19, this suggests that clusters #20 to
 228 24 correspond to root stele cell-types (Figure 2A). Besides, *MtYUC8* and *MtABCG20* genes that
 229 are active in the vascular bundle of the Medicago root (Pawela et al., 2019; Schiessl et al., 2019),
 230 were mostly expressed in cluster #25 (Figure 2A). Taken together, this supports the annotation of
 231 cluster #20 as the Medicago pericycle cell cluster, and of clusters #21 to 25 as Medicago root
 232 vasculature cell-type clusters. Finally, the expression pattern of *MtSUNN*, a receptor-like kinase
 233 acting in the Autoregulation of Nodulation (AON) pathway specifically expressed in the phloem
 234 (Schnabel et al., 2012), precisely maps to cluster #25, thus refining its annotation as the phloem
 235 cells cluster, and the *MtRDNI* AON-related enzyme modifying CLE signaling peptides (Kassaw
 236 et al., 2017) to cluster #24, thus refining its annotation as a xylem cells cluster (Figure 2A).

237

238 **Use of Medicago orthologs of Arabidopsis root cell-type markers for a more exhaustive** 239 **functional annotation of clusters**

240 To further support the functional annotation of these Medicago root clusters, we
 241 additionally analyzed the transcriptional activity of Medicago genes orthologous to 1,086
 242 Arabidopsis root cell-type marker genes (Supplemental Table 3), assuming the conservation of
 243 their cell-type-specific/-enriched transcriptional patterns. Among these genes, 101 were previously
 244 validated markers (Böhme et al., 2004; Denyer et al., 2019; Fendrych et al., 2014; Jean-Baptiste
 245 et al., 2019; Olvera-Carrillo et al., 2015; Ryu et al., 2019; Shulse et al., 2019; Turco et al., 2019;
 246 Zhang et al., 2019) [see (Farmer et al., 2021) for an exhaustive list], 324 were identified in at least
 247 two independent Arabidopsis root single-cell RNA-seq studies (Denyer et al., 2019; Jean-Baptiste
 248 et al., 2019; Ryu et al., 2019; Shulse et al., 2019; Zhang et al., 2019), and 868 genes were identified

249 as the most specifically expressed genes within the 21 sNucRNA-seq clusters of the Arabidopsis
250 root (Farmer *et al.*, 2021). We found that 196 Medicago orthologs share microsyntenic
251 relationships with the 1,086 Arabidopsis root cell-type-specific marker genes thanks to the
252 Comparative Genomic database [CoGe; <https://genomeevolution.org/coge/>; (Lyons and Freeling,
253 2008; Lyons *et al.*, 2008)]. Among these 196 genes, 38 (19.4%) and 58 (29.6%) genes were very
254 low/not expressed, or ubiquitously expressed across all Medicago root clusters, respectively. In
255 the end, we considered 100 Medicago genes orthologous to root cell-type-specific Arabidopsis
256 marker genes to annotate Medicago root clusters (Supplemental Table 4).

257 Among these 100 genes, 10, 2, and 4 are orthologous to Arabidopsis trichoblast-,
258 atrichoblast-, and root cap-specific marker genes, respectively, including the *MtPT1* gene (Chiou
259 *et al.*, 2001) (Supplemental Table 2). Nine trichoblast-specific genes are mostly expressed in
260 cluster #3, whereas *MtPT1* and the remaining six atrichoblast markers are most expressed in
261 clusters #1, 2, 4, and 5 (Figure 2B). This conclusion is further supported by the transcriptional
262 activity in cluster #3 of the *MtLAT52/POE_9* and *MtERN3* genes orthologous to the soybean root-
263 hair-specific *Glyma.18G025200* and *Glyma.05G157400/Glyma.08G115000* genes (Qiao *et al.*,
264 2017), respectively (Figure 2B). Using the same approach, we found that the expression pattern of
265 other Medicago genes orthologous to Arabidopsis cell-type marker genes similarly supported the
266 annotation of the different Medicago root cell-type clusters. The “stem cell niche” annotation was
267 confirmed for cluster #9 based on the transcriptional activity of nine Medicago genes orthologous
268 to Arabidopsis root meristematic genes (Franssen *et al.*, 2015) (Figures 2B, dark grey). Confirming
269 the expression of the endodermis-specific *MtSCR* gene in clusters #17 to 19 (Figure 2B, pink), we
270 additionally identified 23 Medicago genes orthologous to Arabidopsis endodermal cell-specific
271 genes strongly expressed in clusters #15 to 19 (Figure 2B, pink). The annotation of clusters #20 to
272 25 as stele cells was also confirmed based on the transcriptional activity of 49 orthologous genes
273 in these clusters. Among them, xylem (i.e., clusters #22, 23, and 24) and phloem cells (i.e., cluster
274 #25) were identified based on the expression of 23 and 6 Medicago genes orthologous to
275 Arabidopsis xylem- and phloem-specific genes, respectively (Figure 2B, brown and light brown).
276 As a note, three genes orthologous to Arabidopsis xylem marker genes (i.e.,
277 *MtrunA17Chr2g0282871*, *MtrunA17Chr2g0324131*, and *MtrunA17Chr3g0127561*) were also
278 expressed in clusters #4 and 5. We assume that their activity in these two root epidermal cell
279 clusters could reflect the induction of the cell-death program, which was previously reported to be

280 shared between xylem and root cap cells (Farmer *et al.*, 2021; Heo *et al.*, 2017; Kumpf and
281 Nowack, 2015), refining the annotation of clusters #4 and 5 as containing root cap cell-types.
282 Finally, the transcriptional activity of three Medicago genes orthologous to Arabidopsis cortical
283 cell-specific genes in cluster #7 (Figure 2B, grey) suggests that it is composed of developing
284 cortical cells. This result is further supported by the activity of the cortical cell-specific *MtIFS3*
285 and *MtPAL5* genes in cluster #7 (Figure 2B, purple).

286 Taken together, the combined use of previously characterized Medicago root cell-type
287 marker genes with the analysis of the transcriptional activity of Medicago genes orthologous to
288 Arabidopsis root cell-type marker genes led to the functional annotation of 19 out of the 25
289 Medicago root cell clusters of the UMAP (Figure 2A). To annotate the remaining six clusters (#6,
290 8, 10, 11, 12, and 13), all located at the center of the UMAP, we conducted a correlation analysis
291 between the different Medicago root cell clusters, hypothesizing that two clusters sharing highly
292 correlated transcriptomic profiles would relate to the same cell-type. As expected, this analysis
293 revealed several high correlation scores such as between the root epidermal clusters #1 and 2, and
294 for stele/pericycle clusters #20, 21, and 23 (Supplemental Figure 3, highlighted in orange and red
295 squares, respectively). As a note, the remaining non-annotated cluster #8 did not share a correlation
296 with any other cluster, suggesting that cells composing this cluster have a very different
297 transcriptomic profile compared to all other clusters. However, we were able to associate cluster
298 #8 with an intense activity of mitochondrial and ribosomal genes (Supplemental Table 5;
299 Supplemental Figure 4). Previous studies linked the high expression of ribosomal genes with plant
300 developmental processes in maize, Arabidopsis, and tobacco plants (Makabe *et al.*, 2017; Ponnala
301 *et al.*, 2014). These results thus suggest that cluster #8 is composed of cells with high biological
302 activity. Interestingly, we found high correlation scores between clusters #6, 7, 10, 11, 12, 13, and
303 14 (Supplemental Figure 3, yellow squares). As the cell-type marker-based analyses identified
304 clusters #7 and 14 as cortical cells, we assume that clusters #6, 10, 11, 12, and 13 are also composed
305 of cortical cells (Figure 2A), potentially at different stages in their differentiation process and/or
306 corresponding to different layers of the cortex, knowing that there are 4 to 5 layers of cortical cells
307 in *M. truncatula* roots.

308

309 **Conservation of expression patterns between orthologous Arabidopsis and Medicago genes**
310 **at the single-cell level**

311 The previous Arabidopsis-Medicago comparative genomic and transcriptomic analysis
312 used to annotate Medicago root clusters (Figure 2) suggested that transcriptional patterns of
313 orthologous genes could be largely conserved upon speciation of the two plants 108 million years
314 ago (Zeng et al., 2017). To further explore the extent of this conservation at the single-cell level, a
315 correlation analysis was conducted on 3,921 pairs of orthologous genes sharing microsyntenic
316 relationships based on the CoGe database (Lyons and Freeling, 2008; Lyons *et al.*, 2008)
317 (Supplemental Table 6). To maximize the biological significance of the analysis, we processed the
318 previously generated Arabidopsis sNucRNA-seq datasets (Farmer *et al.*, 2021) similarly to the
319 Medicago sNucRNA-seq datasets (see Methods). This updated analysis led to the identification
320 and re-annotation of 16 Arabidopsis root clusters (Farmer *et al.*, 2021) (Figure 3A). We observed
321 a similar topology between the Medicago and Arabidopsis sNucRNA-seq UMAPs (Figures 2A
322 and 3A), with the stem cell niche (#9) located in a star-shaped cluster at the center of the UMAP
323 projection whereas the most differentiated cell-types [e.g. epidermal (#1, 2, and 3), phloem (#25),
324 xylem cells (#22, 23, and 24)] were retrieved in the periphery. To evaluate the conservation of the
325 transcriptional profiles between Arabidopsis and Medicago orthologs, the average gene
326 transcriptional activity of one-to-one orthologs was similarly calculated for each of the 25 mock-
327 inoculated Medicago (Figures 1A) and of the 16 Arabidopsis root clusters (Figure 3A), and a
328 correlation analysis was then conducted (Figure 3B). Stem cell niche (#9; Figure 3B, black square)
329 and stele cells (#20 to 25; Figure 3B, peach-orange square) shared the highest correlation between
330 the two species, suggesting that the transcriptional activities of orthologous genes were most
331 conserved across these root cell-types. To a lesser extent, the transcriptomic profiles of orthologous
332 genes were also conserved between the two species in trichoblasts/epidermal root hair cells (#1 to
333 3; Figure 3B, blue square). Similar conservation was recently reported for root hair, xylem, and
334 phloem cells between the more distantly related rice and Arabidopsis roots (Liu et al., 2021; Zhang
335 et al., 2021). We hypothesize that the unique functions of vascular tissues (xylem and phloem) and
336 trichoblast cells for plant nutrition, as well as the role of the stem cell niche in root development,
337 favored the evolutionary conservation of a core transcriptome between these plant species. In
338 contrast, the transcriptomes of endodermal (#15 to 19) and cortical cell-types (#6, 7, and 10 to 14)
339 were most divergent between Arabidopsis and Medicago (Figure 3B, purple and violet squares),
340 suggesting either difference in nutrient provision when growing the Arabidopsis and Medicago
341 plants, a lower pressure to maintain the transcriptomic signature of these cell-types between the

342 two species, and/or diverging biological functions of these cell-types between Fabaceae (legumes)
343 and Brassicaceae, such as their differential capacity to interact with soil beneficial microbes
344 through endosymbiosis.

345

346 **A differential transcriptional regulation in response to *E. meliloti* of nodulation and** 347 **hormonal genes depending on cell-types**

348 To date, transcriptomic responses of legume roots to rhizobial inoculation were
349 investigated mainly at the whole root level (Mergaert et al., 2019) or on isolated populations of
350 root hair and epidermal cells (Breakspear *et al.*, 2014; Libault *et al.*, 2009). These bulk analyses
351 however lacked resolution, considering that only a subset of plant cells respond to and are infected
352 by rhizobia and that the transcriptional response of cell-types located deeper within roots cannot
353 be easily assessed. Here, we had a unique opportunity to explore the differential regulation of gene
354 expression across the different cell-types in response to *E. meliloti*.

355 To estimate the percentage of individual Medicago root epidermal cells responding to *E.*
356 *meliloti*, we quantified the number of epidermal root cells (i.e., clusters # 1, 2, and 3, excluding
357 the epidermal/root cap clusters #4 and 5) expressing typical early rhizobial infection marker genes,
358 namely *MtRPG*, *MtFLOT4*, and *MtVPY* (Roy *et al.*, 2019). In *E. meliloti*-inoculated roots, 19.5%
359 (433/2225 epidermal nuclei) of epidermal nuclei expressed at least one of these symbiotic marker
360 genes, whereas only 2.3% (39/1694 epidermal nuclei) were detected in mock-inoculated roots. The
361 increase in the number of rhizobia-responsive epidermal cells upon *E. meliloti* inoculation
362 identified is thus significantly larger than the previously estimated size of the epidermal cells
363 population infected by rhizobia, which was about 1-5 % of root hair cells (Nutman, 1959). These
364 results suggest that only a subset of the transcriptionally-responsive root epidermal cells from these
365 three clusters is effectively infected by rhizobia.

366 To identify the set of Differentially Expressed Genes (DEGs) in response to rhizobium
367 inoculation from each Medicago root cell cluster, we used DEsingle, a bioinformatics package
368 designed to identify DEGs from single-cell RNA-seq datasets (Miao et al., 2018). Using a p-value
369 threshold < 0.05 and a $|\text{Fold Change (FC)}| > 1.5$, we identified a total of 8,513 DEGs (Supplemental
370 Table 7). Focusing on the most transcriptionally responsive clusters (i.e., > 500 DEGs; Figure 4A;
371 Supplemental Table 7, bold characters), the root hair cells cluster #2 was retrieved, as well as the
372 cortical clusters #7 and 11, the endodermal clusters # 15, 16, and 18, and the pericycle cluster #20.

373 This result nicely fits with knowledge previously gained using microscopy during early nodule
374 ontogeny (Xiao et al., 2014), which showed that cellular symbiotic processes mainly affected
375 epidermal and cortical cells, and to a lesser extent, endodermis and pericycle cells. We thus further
376 focused our analysis on these clusters, as well as on genes previously known to be acting in
377 nodulation and/or previously annotated as related to hormonal pathways regulating early
378 nodulation stages (Roy *et al.*, 2019).

379 In the trichoblast cluster #2, several known infection-related genes were retrieved as up-
380 regulated, namely *MtCBS1*, *MtRbohG* and *MtRbohH* (Montiel et al., 2018), *MtRPG*, *MtVPY*,
381 *MtAnn1* (de Carvalho Niebel et al., 1998), and *MtNMNI* [i.e., an ortholog of *GmNMNI* (Libault
382 et al., 2011)]. Other genes that belong to the NF signaling pathway were also up-regulated in root
383 hair and epidermal cells in response to *E. meliloti*, namely *MtNFH1*, *MtLYK10* (Larrainzar *et al.*,
384 2015), *MtPUB1* (noting that *MtPUB2* is repressed in this same cluster), *MtIPD3*, *MtDMI1*,
385 *MtDMI2*, *MtDMI3*, *MtNSP1*, *MtNSP2*, *MtERN1*, *MtERN2* (Cerri et al., 2016), and *MtNIN*
386 (Supplemental Tables 8 and 9, Figure 5). Unexpectedly, *MtKNOX3* and *MtKNOX5* genes,
387 previously proposed to control nodule development (Di Giacomo *et al.*, 2017; Dolgikh et al.,
388 2020), and *MtDNF2* [*Does Not fix Nitrogen 2* (Bourcy et al., 2013)] and *MtNCR112* [*Nodule*
389 *Cysteine Rich peptide 112* (Alunni et al., 2007)] genes, regulating later stages of the nodulation
390 process, were also upregulated in cluster #2 48 hours after rhizobium inoculation. In addition, we
391 noticed that *MtNF-YA2* and *MtNF-YA6* genes, phylogenetically related to the early nodulation
392 *MtNF-YA1* gene (Baudin et al., 2015), were also upregulated in cluster #2. Genes belonging to
393 hormonal regulatory pathways were also induced in this cluster in response to rhizobial
394 inoculation. These include notably cytokinin [e.g., *MtIPT1*, *CYP735A1-like*, *MtHPT1*, *MtRRB6*,
395 *MtRRA2*, and *MtRRA5* (Azarakshsh et al., 2018; Tan et al., 2019)] and gibberellin [*MtCPS1*,
396 *MtGA2ox10*, *MtGA3ox1*, and *MtDELLA2*; (Fonouni-Farde et al., 2016; Kim et al., 2019)]
397 biosynthesis and signaling genes. In addition, the expression of genes related to the jasmonic acid
398 [*MtLOX6* (Gao et al., 2007), and *MtJAZ3* (Ge et al., 2016)], auxin [*MtARF10*; (Shen et al., 2015)],
399 abscisic acid [*MtABI5*; (Verdier et al., 2013)], strigolactone [*MtD27*, *MtMAX1a*; (Liu et al., 2011;
400 Müller et al., 2019)], ethylene [*MtETR4* (Tan *et al.*, 2019)], and brassinosteroid [*MtBAK1*
401 (Tavormina et al., 2015)] pathways were also upregulated upon rhizobium inoculation in cluster
402 #2. Conversely, the expression of several genes encoding signaling peptides was repressed by
403 rhizobium in cluster #2, such as *MtPIP1*, *MtIDA20*, *MtIDA31*, and *MtIDA35* (Inflorescence

404 Deficient in Abscission) (de Bang et al., 2017) (Supplemental Tables 8 and 9, Figure 5). To further
 405 estimate the relevance of the trichoblast DEGs identified, we conducted a comparative analysis
 406 with the list of 267 DEGs previously reported in the Medicago root hair cells in response to
 407 rhizobium inoculation (Breakspear *et al.*, 2014). We found that 99 of these genes (37%) were
 408 differentially expressed in the sNucRNA-seq dataset and, among them, 68 genes (69%) were
 409 significantly differentially expressed in at least one of the epidermal clusters #1, 2, or 3
 410 (Supplemental Figure 5). Considering the difference in sensitivity between the technologies used,
 411 these results overall support the identification of genes differentially expressed in Medicago
 412 trichoblasts in response to rhizobia inoculation.

413 The cortical cell cluster #7 DEGs are all repressed upon rhizobium inoculation, including
 414 one gene, *MtCASTOR*, homologous to an *L. japonicus* nodulation gene (Charpentier et al., 2008),
 415 several cytokinin-related genes (two *LOG-like* genes and two *RRA* signaling genes, *MtRRA4* and
 416 *MtRRA9*), the gibberellin signaling gene *MtDELLA1*, and the abscisic acid signaling gene *MtABI5*
 417 (Supplemental Tables 8 and 9, Figure 5). Conversely, the cortical cell cluster #11 DEGs are all
 418 upregulated and include several genes controlling the rhizobia-infection process (*MtRbohA*
 419 (Marino *et al.*, 2011), *MtRbohB*, *MtLIN*), NF signaling (*MtPUB2*, *MtDMI1*, *MtDMI3*, *MtERN2*),
 420 and nodule development [*MtSHR1*, *MtKNOX4* and *MtKNOX9* (Di Giacomo *et al.*, 2017),
 421 *MtNOOT1*, *MtCCS52a* (Cebolla et al., 1999)] and function [*MtNAC969* (de Zélicourt et al., 2012)]
 422 (Supplemental Tables 8 and 9, Figure 5). In addition, hormonal genes related to cytokinin
 423 [*MtCHK1/MtCRE1* (Gonzalez-Rizzo *et al.*, 2006), *MtHPT3*, *MtRRB5*, *MtRRB8*, *MtRRA5*], auxin
 424 (*MtARF10*, *MtARF13*, *MtARF24*), gibberellin (*MtDELLA2*), ethylene (*MtETR1*, *MtEIN3-like*),
 425 jasmonic acid (*MtLOX3*, *MtLOX6*), and strigolactone (*MtMAX2b*), were also upregulated upon
 426 rhizobium inoculation in cluster #11. Finally, two nitrate signaling-related TFs were upregulated
 427 [*MtNLP1* and *MtNLP4* (Luo et al., 2021)] as well as a specific signaling peptide (*MtRTF/DVL11*),
 428 in agreement with the symbiotic function previously reported for *MtDVL1* (Combiér et al., 2008)
 429 (Supplemental Tables 8 and 9, Figure 5). Of note, despite the opposite transcriptional responses
 430 between clusters #7 and 11 to rhizobial inoculation, 232 genes out of the 736 DEGs in cluster #7
 431 (31.5%) were shared as significantly differentially expressed with cluster #11 (Figure 4B). This
 432 indicates that an unexpectedly high number of genes show opposite transcriptional regulation in
 433 response to rhizobium within different cortical cell clusters. This exemplifies that reaching a cell-
 434 type specific level allows identifying that strong up- or down-regulations can occur simultaneously

435 in different clusters at the same 48 hours post-rhizobium inoculation time-point, which would be
436 thus likely missed if whole roots would be used. In addition, the differential transcriptional
437 responses observed between cortical cell clusters for several hormonal pathways and root/nodule
438 developmental genes upon rhizobial inoculation might mark cells that are activated for nodule
439 organogenesis from those that are not, and may relate to the different layers of cortex (i.e. inner
440 *versus* outer), or correspond to cortical cells opposite to proto-phloem *vs* proto-xylem poles where
441 nodule organogenesis is differentially initiated (Heidstra et al., 1997).

442 The endodermal clusters #15, 16, and 18, showing more than 500 DEGs, once more
443 comprise either only downregulated genes (#15 and 18), or upregulated genes for cluster #16
444 (Figure 4A; Supplemental Table 7). In contrast to the cortical cell clusters, these endodermal
445 clusters shared a limited number of DEGs (Figure 4C). Surprisingly, among clusters #15 and 18
446 downregulated genes, many early nodulation genes were observed, including for cluster #15 the
447 infection-related genes *MtLIN*, *MtPUB2*, *MtENODL13*, the NF signaling-related gene *MtDMI2*,
448 the cytokinin signaling genes *MtCHK1/MtCRE1* and *MtRRA2*, as well as the late nodulation genes
449 *MtZPT2-1* (Frugier et al., 2000) and *MtDNF2*; and for cluster #18, the NF signaling gene *MtDMI3*,
450 the cytokinin signaling gene *MtRRB24*, the late nodulation genes *MtZPT2-1* and *MtZPT2-2*, and a
451 signaling peptide, *MtPIPI* (Supplemental Tables 8 and 9, Figure 5). Concerning endodermis
452 cluster #16 upregulated genes, the symbiotic-related gene *MtCASTOR* was retrieved, as well as
453 several hormone-related genes including *MtARF2* and *MtARF8* (auxin), *MtDELLA1* and
454 *MtDELLA2* (gibberellin), *MtRRB9* (cytokinin), *MtEIN3* (ethylene), and the co-receptor *MtBAK1*.
455 In addition, the expression of the nitrate signaling-related *MtNLP1* gene was induced
456 (Supplemental Tables 8 and 9, Figure 5).

457 Finally, in the pericycle (cluster #20), whereas the rhizobium-induced genes do not include
458 any previously studied early nodulation genes, the *MtNRLK1* receptor-like kinase gene (Laffont et
459 al., 2018) was retrieved as slightly induced in response to rhizobia. The *MtRbohG*, *MtENOD40*,
460 *MtZPT2-1*, and *MtZPT2-2* nodulation genes were unexpectedly repressed by rhizobium, as well as
461 the *MtKNOX9* developmental gene. Regarding hormonal-related genes, the cytokinin *MtRRB5*, the
462 auxin *MtYUC8*, and the ethylene *MtEBF1* gene, as well as the *MtIDA33* signaling peptide and the
463 *MtSERK* co-receptor, were also repressed (Supplemental Tables 8 and 9, Figure 5).

464 Taken together, our unique dataset allowed a refined expression pattern analysis which
465 revealed unexpected cell-type specificity/enrichment for some of the already well-known early

466 nodulation genes (e.g., a differential expression across cortical cell clusters and repression in
 467 endodermal cell clusters) or for the *MtCASTOR* gene which currently has no symbiotic function
 468 reported in *M. truncatula* unlike its homolog from *L. japonicus* (Venkateshwaran et al., 2012). In
 469 addition, some nodulation genes that were previously linked to later symbiotic stages (e.g.,
 470 *MtNCR112*, *MtZPT2-1*, *MtZPT2-2*, *MtDNF2*, *MtNAC969*) also showed a differential expression
 471 in response to rhizobium in specific root cell-type clusters. Surprisingly, a few anticipated early
 472 nodulation genes were missing from the DEG dataset (e.g. *MtLIN*, *MtNF-YA1*, *MtNPL*), but a
 473 manual inspection of their expression profiles revealed differential regulations by rhizobia that
 474 were below the statistical threshold used. This indicates that our statistical analysis is conservative,
 475 allowing providing a robust dataset of DEGs, but also likely missing other genes of interest. More
 476 refined statistical analyses could be however performed in the future on this dataset, focussing
 477 only on a subset of specific clusters to extract such additional information that is currently lost due
 478 to the high variance between all nuclei analyzed.

479

480 **Cell-type-specific expression of nodulation and cytokinin-signaling related genes**

481 As many nodulation-related genes can be already expressed in cells prior to bacterial
 482 inoculation, we additionally conducted a comprehensive analysis of their expression patterns
 483 independently of their response to rhizobial inoculation, focusing notably on genes showing cell-
 484 type-enriched or -specific patterns that were not previously identified as DEGs (see above).
 485 Epidermal cells (#1 to 5) most specifically expressed the *MtROP5* (Riely et al., 2011), *MtLIN*, and
 486 *MtPT5* (Wang et al., 2022) genes associated with rhizobial infections (clusters #2 and 3) (Damiani
 487 et al., 2016); *MtNFP*, *MtLYK3* (Smit et al., 2007), *MtLYK6*, *MtCNGC15c* (Charpentier et al.,
 488 2016), and *MtNF-YA1* genes, related to NF signaling (clusters #2 and 3); *MtCHIT5a* that is linked
 489 to NF degradation [clusters #4 and 5; (Tian et al., 2013)]; as well as genes related to late nodulation
 490 stages, namely *MtRab7A1* (Limpens et al., 2009), *MtSYP132* (Pan et al., 2016), *MtVPE*, *MtSPK1*
 491 (Andrio et al., 2013), *MtZIP6* (Abreu et al., 2017) (clusters #2 and 3), *MtDNF2* (cluster #4),
 492 *MtDGD1* (Si et al., 2019) (clusters #4 and 5), and *MtNAC969* (cluster #5); and *MtNLP1*, a gene
 493 linked to nitrate signaling (clusters #2 and 3) (Figure 6A).

494 In contrast, only a small number of previously characterized nodulation-related genes were
 495 specifically expressed/enriched in the non-annotated cluster #8, in the stem cell niche cluster #9,
 496 and in the cortical clusters #6, 7, and 10 to 14 [i.e., *MtCHK1/CRE1*, a cytokinin receptor required

497 for nodule organogenesis in cluster #7; *MtLATD/NIP*, an abscisic acid transporter linked to early
 498 nodulation in cluster #8 (Bagchi et al., 2012); *MtBR11*, a brassinosteroid receptor linked to
 499 nodulation (Cheng et al., 2017), and *MtPIN2*, an auxin efflux carrier linked to nodule
 500 organogenesis in cluster #9 (Huo et al., 2006); and *MtGlb1-1*, a gene involved in later nodulation
 501 stages in cluster #11 (Berger et al., 2020)] (Figure 6B).

502 In the endodermis (#15 to 19), we identified several nodulation-related genes specifically
 503 expressed in one or several clusters [i.e., *MtKNOX5* (cluster #16), *MtRbohG*, *MtZPT2-1*, and
 504 *MtCDPK1* (cluster #18, as well as in the cortical cell cluster #14, (Ivashuta et al., 2005)),
 505 *MtCDPK3* (clusters #18 and 19), *MtKNOX3* (clusters #16 and 19), *MtANN1* (clusters #15 and 19),
 506 *MtDMI3* (cluster #19 in addition to the epidermal cell clusters #1, 2, and 3), *MtSYT3* (Gavrin et
 507 al., 2017), *MtTOP6A* (an ortholog to *LjSUNERGOS1* (Yoon et al., 2014)), and *MtMAPK6* (cluster
 508 #19; (Chen et al., 2017))] (Figure 6C).

509 In the stele (#20 to 25), a *LjTRICOT-like* gene (Suzaki et al., 2013), *MtMATE69* (Wang et
 510 al., 2017), and *MtTML2* (Gautrat et al., 2019) were specifically expressed in cluster #20 (pericycle
 511 cells) while *MtDNF1* (Van de Velde et al., 2010; Wang et al., 2010), *MtVAMP721a* (Sinharoy et
 512 al., 2013), *MtPIN3* (Huo et al., 2006), *MtRab7a2* (Limpens et al., 2009), *MtSUC1* (Hohnjec et al.,
 513 2003), *MtARP3* (Gavrin et al., 2015), *MtSYT1* (Gavrin et al., 2017), TOR-like, *MtCDC16*
 514 (Kuppusamy et al., 2009), *MtKNOX9*, *MtPIN4* (Huo et al., 2006), *MtEFD* (Vernié et al., 2008),
 515 *MtLAX2* (Roy et al., 2017), *MtTPS2*, *MtVAMP721d* (Ivanov et al., 2012), *MtNF-YC2* (Baudin et
 516 al., 2015), *MtCCS52a*, and *MtRDN1* (Schnabel et al., 2011) were enriched in at least one of the
 517 xylem clusters (i.e., #22 to 24). Finally, in cluster #25 (phloem), we identified several genes
 518 associated with the systemic regulation of nodulation (Gautrat et al., 2021), namely *MtCRA2*
 519 (Huault et al., 2014; Mohd-Radzman et al., 2016), *MtSUNN*, *MtTML1* (Gautrat et al., 2019),
 520 *MtIPT3*, and *MtMPKK5* (Figure 6D). These observations are well supported by previous studies
 521 reporting the cell-type specificity of these genes.

522 Considering the cytokinin signaling pathway which is key for early nodulation (Gamas et
 523 al., 2017), we found *MtRRA5* most expressed in epidermal clusters #1 to 3, as well as in clusters
 524 #7 (cortex) and 19 (endodermis), *MtRRA2* in clusters #2 and 3 (epidermis/root hairs), *MtRRA11* in
 525 clusters #3 (epidermis) and 7 (cortex), *MtCHK1/CRE1*, *MtCHK4*, *MtHPT8*, and *MtRRA4* in cluster
 526 #7 (cortex), *MtCHK2* and *MtHPT3* in clusters #17 and 18 (endodermis), *MtRRB5* in cluster #18
 527 (endodermis), *MtRRB1*, *MtRRA3*, *MtRRA4*, *MtRRA6* and *MtRRA8* in cluster #20 (pericycle),

528 *MtHPT8* and *MtRRA9* in clusters #22, 23, and 24 (xylem), and *MtCHK3*, *MtHPT1*, *MtHPT4*,
529 *MtRRB4* and *MtRRB20* in cluster #25 (phloem) (Figure 6E).

530 These results overall support that many early nodulation genes, including those involved
531 in cytokinin signaling, have a cell-type specific/enriched expression pattern, indicating a
532 coordinated activity between cell-types to successfully promote nodule initiation. Interestingly,
533 the co-regulation in a specific cluster of different genes belonging to a large family, or even to the
534 same functional pathway, combined with phylogenetic analyses, now provides critical information
535 to develop more efficient functional analyses to overcome functional redundancy. As an example,
536 the *RRB* family related to cytokinin signaling contains 12 genes for which expression was detected
537 in at least one cluster of the UMAP. Noteworthy, *MtRRB4* and *MtRRB20* have overlapping
538 expression patterns in the phloem (cluster #25), suggesting a likely functional redundancy, also
539 knowing their close phylogenetic relationship in the same clade (Tan *et al.*, 2019). When
540 combining this information with the expression pattern of genes from other cytokinin signaling
541 families, a specific cytokinin signaling pathway preferentially acting in the phloem cells can now
542 be identified, involving the *MtCHK3* receptor, the *MtHPT1* and *MtHPT4* phosphotransfer
543 proteins, and the *MtRRB4* and *MtRRB20* TFs. Similarly, when considering systemic pathways
544 regulating nodulation (Gautrat *et al.*, 2021), our analysis strikingly demonstrates that most known
545 genes (i.e. *MtCRA2*, *MtSUNN*, *MtIPT3*, *MtTML1*) are specifically expressed, and even induced by
546 rhizobium in phloem cells (cluster #25). Importantly, getting access to such very detailed and
547 clearcut spatial expression information allows generating innovative working hypotheses to be
548 further tested functionally.

549

550 **Root cell-type specific vs shared functional pathways enriched in response to a short-term** 551 **rhizobium inoculation**

552 To reveal new biological functions potentially controlling the response of *Medicago* root
553 cell-types to *E. meliloti*, we performed a gene ontology analysis using the Mapman software
554 (Schwacke *et al.*, 2019; Tellström *et al.*, 2007) on the DEGs from clusters #2, 7, 11, 15, 16, 18, 20
555 containing more than 500 DEGs (Figure 4A). The full list of enriched functional pathways is
556 shown in Supplemental Table 10 and Supplemental Figure 6.

557 In cluster #2, functional pathways corresponding to changes in cellular organization,
558 including modification of the cell wall (pectin esterases) and vesicle transport were enriched for

559 genes upregulated in response to bacterial inoculation (Wilcoxon rank-sum test, $p < 0.05$). This
560 likely reflects the curling of root hairs associated with rhizobial infections. Among metabolic
561 pathways, the flavonoid metabolism was enriched, notably the biosynthesis of dihydroflavonols,
562 as well as the cytokinin and gibberellin biosynthesis pathways. This result strikingly fits with
563 knowledge gained during the last decades where these three plant signaling pathways were shown
564 as crucial for the regulation of early stages of rhizobial infections in the *Medicago* root epidermis
565 (Fonouni-Farde et al., 2017; Fonouni-Farde *et al.*, 2016; Gonzalez-Rizzo *et al.*, 2006; Plet *et al.*,
566 2011; Roy *et al.*, 2019). In addition, both lysine motif and leucine-rich repeats receptor kinases
567 were enriched in this trichoblast cluster #2 in response to rhizobium inoculation, which includes
568 already known receptors required for rhizobial recognition and infection, as well as the
569 phosphoinositide metabolism and PHD finger or GRAS TFs, the latter family including also already
570 known early nodulation genes. Concerning genes downregulated by rhizobia, the brassinosteroid
571 and ethylene pathways were enriched, the latter hormone being previously extensively
572 characterized as an inhibitor of rhizobial infections, notably in *Medicago* (Penmetsa et al., 2008).

573 Cortical cell clusters #7 downregulated DEGs showed enrichment for cell wall
574 modifications and lipid metabolism, several hormonal pathways namely abscisic acid metabolism,
575 ethylene signaling, as well as AP2/EREBP and Trihelix TF families; and cluster #11 upregulated
576 DEGs for biotic stress responses, lipid, terpenoid, phenylpropanoid and glucosinolate metabolic
577 functions, as well as C2H2 zinc finger, CCAAT box binding factors, G2-like (GARP), and MYB-
578 related TF families, the protein targeting secretory and protein degradation pathways (subtilases
579 and autophagy), and cytoskeleton reorganization.

580 Endodermal cells clusters #15 and 18 (downregulated genes) were enriched for cell wall
581 degradation and lipid metabolism functions, as well as ethylene and jasmonate metabolism, GRAS
582 TF families, leucine-rich repeat receptor kinases, and protein degradation via ubiquitination.
583 Regarding cluster #16 (upregulated genes), the biotic stress response and glucosinolate
584 degradation functions were enriched, as well as the jasmonate hormone and the ARR TF family
585 related to cytokinins, cell division and cell cycle, and sugar transport.

586 Finally, in pericycle cells (cluster #20), rhizobium downregulated genes were once more
587 enriched for ethylene signaling pathway genes and AP2/EREBP TFs, as previously observed for
588 the root hair cluster #2, the cortex cluster #7, and the endodermal clusters #15 and 18, highlighting
589 one of the few shared biological responses across different cell-types.

590 Overall, as previously noticed for the analysis of known nodulation-related genes, the novel
591 cell-type specific information gained allows for generating new hypotheses, such as the existence
592 of a tight interaction in inner root tissues of symbiotic responses with defense pathways through
593 the modulation of specific specialized metabolite production. It also highlights specific hormonal
594 pathways and TF families for which functional studies remain still limited, or even lacking, and
595 that could thus be targeted in the future in relation to cell-type specific phenotypes (e.g. rhizobial
596 infections or nodule organogenesis).

597

598 **Conclusions**

599 Plant root development requires tightly coordinated regulation of transcriptomic programs.
600 We and others revealed root transcriptomic profiles at a single-cell level notably in the model plant
601 *A. thaliana* (Denyer *et al.*, 2019; Farmer *et al.*, 2021; Jean-Baptiste *et al.*, 2019; Ryu *et al.*, 2019;
602 Shulse *et al.*, 2019; Zhang *et al.*, 2019). In this study, we provide a comprehensive annotation of
603 the Medicago root cell-types according to their transcriptomic profiles, as well as an analysis of
604 the transcriptomic response of Medicago root cells to rhizobial infection. Our study largely
605 confirmed knowledge gained during the last decades in legume nodulation (i.e., the regulation of
606 the expression of nodulation-related and hormonal genes known to regulate rhizobial infection
607 and/or nodule organogenesis), but also nicely illustrates the gain of knowledge obtained using such
608 single nuclei transcriptomic approaches to better understand the cell-type specifically restricted
609 responses of plants to microbial infection. The robust and high-quality dataset generated is also a
610 resource to enable the discovery of new genes of interest not previously highlighted by bulk
611 transcriptomic analyses. In particular, accessing cell-type information allows for generating more
612 precise hypotheses regarding the symbiotic processes potentially affected by these novel candidate
613 DEGs, and thus facilitates planning more appropriately experimental designs, notably by using
614 tissue-specific promoters for which single-cell datasets are a key resource, and for performing
615 refined focused phenotyping of rhizobial infections *versus* nodule organogenesis. We foresee that
616 the application of single-cell -omics technologies to other symbiotic and pathogenic plant-microbe
617 interactions will lead to a better understanding of the intimate complexity of the relationships
618 between plants and microbes.

619

620 **Methods**

621 Plant materials, root nucleus isolation, library preparation, and sequencing

622 Medicago seedlings were sterilized as described in Pingault et al., 2018. Eight seeds were
623 then placed on agar B&D medium (Broughton and Dilworth, 1971) without nitrogen, and placed
624 in a growth chamber in the dark for four days (26 °C for 16h and 20 °C for 8h). On the fourth day,
625 four mL of an *E. meliloti* suspension (OD_{600nm}=0.1), or water for the mock-inoculated samples,
626 were applied to the seedlings' roots. The plates were placed back into the growth chamber for 48
627 hours in the dark. On the sixth day, a subset of the *E. meliloti*-inoculated plants was transferred in
628 vermiculite:perlite (3:1) and grown in the growth chamber (16 hours daylight) for three weeks to
629 confirm rhizobial infection and the formation of nodules. The remaining roots were used to collect
630 the nuclei as described in Thibivilliers et al., 2020. The root samples used for these experiments
631 were around 3 to 4 cm long, starting from the tip and ending in the zone where root hairs are fully
632 differentiated, thus including the zone susceptible to rhizobial infection. Briefly, roots were then
633 chopped and passed through a 30µm cell strainer. The filtered nuclei were purified by cell sorting
634 using FACS Aria II™ cell sorter (BD Biosciences). An average of 80-100,000 nuclei were
635 collected for each sample, centrifuged, and re-suspended in phosphate buffered saline-bovine
636 serum albumin 0.5%-RNA-inhibitor solution. The six sNucRNA-seq libraries (i.e., three *E.*
637 *meliloti*- and three mock-inoculated root libraries) were constructed following the Chromium™
638 Single Cell 3' Library & Gel Bead Kit v3.1 protocol (10x Genomics). The sequencing of single-
639 indexed paired-end libraries was performed on an Illumina™ NovaSeq 6000 platform according
640 to the 10x Genomics recommendations.

641

642 Pre-processing of raw data, integration, clustering, and annotation. The six Medicago sNucRNA-
643 seq libraries were preprocessed individually using the 10x Genomics Cell Ranger software
644 v6.1.1.0, and then aligned against the latest version of the *Medicago truncatula* reference genome
645 and genome annotation (<https://medicago.toulouse.inra.fr/MtrunA17r5.0-ANR/>) (Pecrix et al.,
646 2018). Upon removal of background contamination using the SoupX software (Young and Behjati,
647 2020), filtration of doublets using the DoubletDetection prediction method (Adam Gayoso, 2022),
648 and applying a statistical threshold on the data distribution (i.e., an interval of confidence of 95%
649 to remove outliers; see Supplemental Figure 1 to access the parameters for each sNucRNA-seq
650 library), the normalization of individual sNucRNA-seq datasets and their respective integration to
651 generate UMAPs was performed using Seurat V4 (Hao et al., 2021), selecting “top 2000 variable

652 genes” for feature selection. Integration anchors were defined for the combined set of six
653 sNucRNA-seq datasets based on the first 20 dimensions of the canonical correlation analysis
654 method. After integration, the dimensionality reduction was performed with the first 40 principal
655 components to generate the UMAP projection. Besides, the clustering was generated with the
656 method FindClusters from Seurat with a resolution of 0.6. For downstream analyses, the
657 expression values of each gene were calculated for each cluster using the AverageExpression
658 function from Seurat.

659 For the annotation of cell-types, the cluster-specific genes were identified with the
660 FindAllMarkers function in Seurat. In addition, the expression patterns of known cell-type specific
661 gene markers from *M. truncatula* (Supplemental Table 2 and Medicago genes orthologous to *A.*
662 *thaliana* root cell-type marker genes were further analyzed (Farmer *et al.*, 2021) (Supplemental
663 Table 4).

664

665 UMAP visualization. For visualization purposes, all sNucRNA-seq libraries were combined
666 using the Cell Ranger aggr function from 10x Genomics to combine all counts in a single cloupe
667 file, and to show the UMAP coordinates projections and cell cluster assignments obtained from
668 the Seurat analysis. We use ShinyCell (available at <https://github.com/SGDDNB/ShinyCell>), a
669 web application allowing the visualization of single-cell data, to allow direct inquiries of the
670 Medicago root single-cell transcriptome atlas (available from the
671 [https://shinycell.legumeinfo.org/medtr.A17.gnm5.ann1_6.expr.Cervantes-](https://shinycell.legumeinfo.org/medtr.A17.gnm5.ann1_6.expr.Cervantes-Perez_Thibivilliers_2022/)
672 [Perez_Thibivilliers_2022/](https://shinycell.legumeinfo.org/medtr.A17.gnm5.ann1_6.expr.Cervantes-Perez_Thibivilliers_2022/) web interface).

673

674 Differential Gene expression analysis. To identify DEGs, raw read counts were extracted to
675 calculate a normalized average expression for each gene, in each cluster, and for each condition
676 (Supplemental Table 9) before applying the DEsingle package (Miao *et al.*, 2018) using p-
677 value<0.05 and $|FC| > 1.5$ thresholds. This package allows the identification of DEGs between
678 *E. meliloti*- and mock-inoculated nuclei in a raw read count matrix employing the Zero-Inflated
679 negative binomial model (Wang *et al.*, 2019).

680

681 Correlation analysis between plant root single nuclei transcriptomes. To support the functional
682 annotation in the *M. truncatula* root clusters, we compared the transcriptomes of the different

683 Medicago root clusters upon extracting the pseudo-bulk expression of each gene among all clusters
684 and then conducted Pearson's correlation analyses to reveal the most similar transcriptomes among
685 all nuclei clusters.

686 To compare the transcriptome of Medicago and Arabidopsis root clusters, *A. thaliana*
687 sNucRNA-seq datasets were obtained from previously published data (Farmer *et al.*, 2021), based
688 on the following SRA files: GSM4698755, GSM4698756, GSM4698757, GSM4698758,
689 GSM4698759. The five replicates were processed individually using the 10x Genomics Cell
690 Ranger v6.1.1.0 pipeline, and then mapped against a reference genome constructed with
691 TAIR10.26 genome and Araport11 annotations. The same parameters were then used for
692 preprocessing the Arabidopsis datasets as previously used for the Medicago sNucRNA-seq
693 datasets (see above). To correlate the *A. thaliana* and *M. truncatula* root sNuc-transcriptomes, we
694 extracted pseudo-bulk information for the one-to-one orthologs between the two plant species
695 [CoGe; <https://genomevolution.org/coge/>; (Lyons and Freeling, 2008; Lyons *et al.*, 2008)] and
696 conducted a Pearson's correlation analysis between the expression of these orthologous genes for
697 each cell cluster.

698
699 *Genes of interest and functional classification analyses.* The Legoo knowledge base ([https://lipm-](https://lipm-browsers.toulouse.inra.fr/k/legoo/)
700 [browsers.toulouse.inra.fr/k/legoo/](https://lipm-browsers.toulouse.inra.fr/k/legoo/)) was used to identify genes of interest (Carrère *et al.*, 2019), as
701 well as the Mapman software (<https://mapman.gabipd.org/>) for the analysis of gene functions
702 (Thimm *et al.*, 2004).

703

704 **Funding**

705 This work was supported by grants to M.L. from the U.S. National Science
706 Foundation (IOS #1854326 and 2127485), USDA-NIFA (#2022-67013-36144), by the Center for
707 Plant Science Innovation, and by the Department of Agronomy and Horticulture at the University
708 of Nebraska-Lincoln. Work in F.F. lab was supported by the "Ecole Universitaire de Recherche"
709 Saclay Plant Sciences (EUR-SPS).

710

711 **Author contributions**

712 S.T. performed experiments. S.A.C.P., S.T., C. L., A.D.F., F.F., and M.L. carried out data
713 analysis. M.L. coordinated the study. S.A.C.P., S.T., F.F., and M.L. drafted the manuscript. All
714 authors contributed to the preparation of the manuscript.

715

716 **Acknowledgments**

717 The authors would like to acknowledge Lana Koepke Johnson from the Department of
718 Agronomy and Horticulture at the University of Nebraska-Lincoln for her artistic work to create
719 Figure 5. We also want to acknowledge Dirk Anderson, manager of the Flow Cytometry Core
720 Facility, the Single Cell Genomics Core Facility, and the Nebraska Center for Biotechnology at
721 the University of Nebraska-Lincoln, for providing support in the sorting of the isolated nuclei and
722 for their processing to generate sNucRNA-seq libraries.

723

724 **Accession numbers**

725 Expression data are available at the Gene Expression Omnibus (GEO: GSE210881). The
726 Medicago root single-cell transcriptome atlas can be accessed through
727 [https://shinycell.legumeinfo.org/medtr.A17.gnm5.ann1_6.expr.Cervantes-](https://shinycell.legumeinfo.org/medtr.A17.gnm5.ann1_6.expr.Cervantes-Perez_Thibivilliers_2022/)
728 [Perez_Thibivilliers_2022/](https://shinycell.legumeinfo.org/medtr.A17.gnm5.ann1_6.expr.Cervantes-Perez_Thibivilliers_2022/).

729

730 **References**

731 **Abreu, I., Saéz, Á., Castro-Rodríguez, R., Escudero, V., Rodríguez-Haas, B., Senovilla, M.,**
732 **Larue, C., Grolimund, D., Tejada-Jiménez, M., Imperial, J., et al. (2017).** *Medicago truncatula*
733 *Zinc-Iron Permease6 provides zinc to rhizobia-infected nodule cells. Plant Cell Environ* **40**:2706-
734 2719. 10.1111/pce.13035.

735 **Adam Gayoso, J.S. (2022).** JonathanShor/DoubletDetection: doubletdetection v4.2 (v4.2).
736 Zenodo. 10.5281/zenodo.6349517.

737 **Alunni, B., Kevei, Z., Redondo-Nieto, M., Kondorosi, A., Mergaert, P., and Kondorosi, E.**
738 **(2007).** Genomic organization and evolutionary insights on *GRP* and *NCR* genes, two large
739 nodule-specific gene families in *Medicago truncatula*. *Mol Plant Microbe Interact* **20**:1138-1148.
740 10.1094/mpmi-20-9-1138.

- 741 **Andrianakaja, A., Boisson-Dernier, A., Frances, L., Sauviac, L., Jauneau, A., Barker, D.G.,**
742 **and de Carvalho-Niebel, F.** (2007). AP2-ERF transcription factors mediate Nod factor dependent
743 MtENOD11 activation in root hairs via a novel cis-regulatory motif. *The Plant cell* **19**:2866-2885.
744 10.1105/tpc.107.052944.
- 745 **Andrio, E., Marino, D., Marmeys, A., de Segonzac, M.D., Damiani, I., Genre, A., Huguet, S.,**
746 **Frendo, P., Puppo, A., and Pauly, N.** (2013). Hydrogen peroxide-regulated genes in the
747 *Medicago truncatula-Sinorhizobium meliloti* symbiosis. *New Phytol* **198**:179-189.
748 10.1111/nph.12120.
- 749 **Ané, J.M., Kiss, G.B., Riely, B.K., Penmetza, R.V., Oldroyd, G.E., Ayax, C., Lévy, J., Debellé,**
750 **F., Baek, J.M., Kalo, P., et al.** (2004). *Medicago truncatula DMII* required for bacterial and fungal
751 symbioses in legumes. *Science* **303**:1364-1367. 10.1126/science.1092986.
- 752 **Arrighi, J.-F., Godfroy, O., Billy, F.d., Saurat, O., Jauneau, A., and Gough, C.** (2008). The
753 *RPG* gene of *Medicago truncatula* controls Rhizobium-directed polar growth during infection.
754 *Proceedings of the National Academy of Sciences* **105**:9817-9822. doi:10.1073/pnas.0710273105.
- 755 **Azarakhsh, M., Lebedeva, M.A., and Lutova, L.A.** (2018). Identification and Expression
756 Analysis of *Medicago truncatula* Isopentenyl Transferase Genes (IPTs) Involved in Local and
757 Systemic Control of Nodulation. *Frontiers in plant science* **9**:304-304. 10.3389/fpls.2018.00304.
- 758 **Bagchi, R., Salehin, M., Adeyemo, O.S., Salazar, C., Shulaev, V., Sherrier, D.J., and**
759 **Dickstein, R.** (2012). Functional assessment of the *Medicago truncatula* NIP/LATD protein
760 demonstrates that it is a high-affinity nitrate transporter. *Plant Physiol* **160**:906-916.
761 10.1104/pp.112.196444.
- 762 **Baudin, M., Laloum, T., Lepage, A., Rípodas, C., Ariel, F., Frances, L., Crespi, M., Gamas,**
763 **P., Blanco, F.A., Zanetti, M.E., et al.** (2015). A Phylogenetically Conserved Group of Nuclear
764 Factor-Y Transcription Factors Interact to Control Nodulation in Legumes. *Plant physiology*
765 **169**:2761-2773. 10.1104/pp.15.01144.
- 766 **Berger, A., Guinand, S., Boscari, A., Puppo, A., and Brouquisse, R.** (2020). *Medicago*
767 *truncatula Phytooglobin 1.1* controls symbiotic nodulation and nitrogen fixation via the regulation
768 of nitric oxide concentration. *The New phytologist* **227**:84-98. 10.1111/nph.16462.
- 769 **Bhuvaneshwari, T.V., Bhagwat, A.A., and Bauer, W.D.** (1981). Transient susceptibility of root
770 cells in four common legumes to nodulation by rhizobia. *Plant Physiol* **68**:1144-1149.

- 771 **Biala, W., Banasiak, J., Jarzyniak, K., Pawela, A., and Jasinski, M.** (2017). *Medicago*
772 *truncatula* ABCG10 is a transporter of 4-coumarate and liquiritigenin in the medicarpin
773 biosynthetic pathway. *Journal of experimental botany* **68**:3231-3241. 10.1093/jxb/erx059.
- 774 **Birnbaum, K., Shasha, D.E., Wang, J.Y., Jung, J.W., Lambert, G.M., Galbraith, D.W., and**
775 **Benfey, P.N.** (2003). A Gene Expression Map of the Arabidopsis Root. *Science* **302**:1956-1960.
776 10.1126/science.1090022.
- 777 **Böhme, K., Li, Y., Charlot, F., Grierson, C., Marrocco, K., Okada, K., Laloue, M., and**
778 **Nogué, F.** (2004). The Arabidopsis *COWI* gene encodes a phosphatidylinositol transfer protein
779 essential for root hair tip growth. *Plant J* **40**:686-698. 10.1111/j.1365-313X.2004.02245.x.
- 780 **Boivin, S., Fonouni-Farde, C., and Frugier, F.** (2016). How Auxin and Cytokinin
781 Phytohormones Modulate Root Microbe Interactions. *Frontiers in plant science* **7**:1240-1240.
782 10.3389/fpls.2016.01240.
- 783 **Bourcy, M., Brocard, L., Pislariu, C.I., Cosson, V., Mergaert, P., Tadege, M., Mysore, K.S.,**
784 **Udvardi, M.K., Gourion, B., and Ratet, P.** (2013). *Medicago truncatula* DNF2 is a PI-PLC-XD-
785 containing protein required for bacteroid persistence and prevention of nodule early senescence
786 and defense-like reactions. *New Phytol* **197**:1250-1261. 10.1111/nph.12091.
- 787 **Breakspear, A., Liu, C., Roy, S., Stacey, N., Rogers, C., Trick, M., Morieri, G., Mysore, K.S.,**
788 **Wen, J., Oldroyd, G.E.D., et al.** (2014). The Root Hair “Infectome” of *Medicago truncatula*
789 Uncovers Changes in Cell Cycle Genes and Reveals a Requirement for Auxin Signaling in
790 Rhizobial Infection *The Plant Cell* **26**:4680-4701. 10.1105/tpc.114.133496.
- 791 **Broughton, W.J., and Dilworth, M.J.** (1971). Control of leghaemoglobin synthesis in snake
792 beans. *The Biochemical journal* **125**:1075-1080. 10.1042/bj1251075.
- 793 **Cai, J., Zhang, L.-Y., Liu, W., Tian, Y., Xiong, J.-S., Wang, Y.-H., Li, R.-J., Li, H.-M., Wen,**
794 **J., Mysore, K.S., et al.** (2018). Role of the Nod Factor Hydrolase MtNFH1 in Regulating Nod
795 Factor Levels during Rhizobial Infection and in Mature Nodules of *Medicago truncatula*. *The*
796 *Plant cell* **30**:397-414. 10.1105/tpc.17.00420.
- 797 **Carrère, S., Verdenaud, M., Gough, C., Gouzy, J., and Gamas, P.** (2019). LeGOO: An
798 Expertized Knowledge Database for the Model Legume *Medicago truncatula*. *Plant and Cell*
799 *Physiology* **61**:203-211. 10.1093/pcp/pcz177.
- 800 **Cebolla, A., María Vinardell, J., Kiss, E., Oláh, B., Roudier, F., Kondorosi, A., and**
801 **Kondorosi, E.** (1999). The mitotic inhibitor *ccs52* is required for endoreduplication and ploidy-

802 dependent cell enlargement in plants. The EMBO Journal **18**:4476-4484.
803 10.1093/emboj/18.16.4476.

804 **Cerri, M.R., Frances, L., Kelner, A., Fournier, J., Middleton, P.H., Auriac, M.C., Mysore,**
805 **K.S., Wen, J., Erard, M., Barker, D.G., et al.** (2016). The Symbiosis-Related ERN Transcription
806 Factors Act in Concert to Coordinate Rhizobial Host Root Infection. *Plant Physiol* **171**:1037-1054.
807 10.1104/pp.16.00230.

808 **Charpentier, M., Bredemeier, R., Wanner, G., Takeda, N., Schleiff, E., and Parniske, M.**
809 (2008). Lotus japonicus CASTOR and POLLUX are ion channels essential for perinuclear calcium
810 spiking in legume root endosymbiosis. *The Plant cell* **20**:3467-3479. 10.1105/tpc.108.063255.

811 **Charpentier, M., Sun, J., Martins, T.V., Radhakrishnan, G.V., Findlay, K., Soumpourou, E.,**
812 **Thouin, J., Véry, A.-A., Sanders, D., Morris, R.J., et al.** (2016). Nuclear-localized cyclic
813 nucleotide-gated channels mediate symbiotic calcium oscillations. *Science* **352**:1102-1105.
814 doi:10.1126/science.aae0109.

815 **Chen, T., Zhou, B., Duan, L., Zhu, H., and Zhang, Z.** (2017). *MtMAPKK4* is an essential gene
816 for growth and reproduction of *Medicago truncatula*. *Physiologia Plantarum* **159**:492-503.
817 10.1111/ppl.12533.

818 **Cheng, X., Gou, X., Yin, H., Mysore, K.S., Li, J., and Wen, J.** (2017). Functional
819 characterisation of brassinosteroid receptor MtBRI1 in *Medicago truncatula*. *Scientific Reports*
820 **7**:9327. 10.1038/s41598-017-09297-9.

821 **Chiou, T.-J., Liu, H., and Harrison, M.J.** (2001). The spatial expression patterns of a phosphate
822 transporter (MtPT1) from *Medicago truncatula* indicate a role in phosphate transport at the
823 root/soil interface. *The Plant Journal* **25**:281-293. 10.1046/j.1365-313x.2001.00963.x.

824 **Combiér, J.-P., Frugier, F., de Billy, F., Boualem, A., El-Yahyaoui, F., Moreau, S., Vernié,**
825 **T., Ott, T., Gamas, P., Crespi, M., et al.** (2006). MtHAP2-1 is a key transcriptional regulator of
826 symbiotic nodule development regulated by microRNA169 in *Medicago truncatula*. *Genes Dev*
827 **20**:3084-3088. 10.1101/gad.402806.

828 **Combiér, J.P., Küster, H., Journet, E.P., Hohnjec, N., Gamas, P., and Niebel, A.** (2008).
829 Evidence for the involvement in nodulation of the two small putative regulatory peptide-encoding
830 genes *MtRALFL1* and *MtDVLI*. *Molecular plant-microbe interactions : MPMI* **21**:1118-1127.
831 10.1094/mpmi-21-8-1118.

- 832 **Cvrčková, F., Bezdová, R., and Zárský, V.** (2010). Computational identification of root hair-
833 specific genes in Arabidopsis. *Plant signaling & behavior* **5**:1407-1418. 10.4161/psb.5.11.13358.
- 834 **Damiani, I., Drain, A., Guichard, M., Balzergue, S., Boscari, A., Boyer, J.C., Brunaud, V.,**
835 **Cottaz, S., Rancurel, C., Da Rocha, M., et al.** (2016). Nod Factor Effects on Root Hair-Specific
836 Transcriptome of *Medicago truncatula*: Focus on Plasma Membrane Transport Systems and
837 Reactive Oxygen Species Networks. *Front Plant Sci* **7**:794. 10.3389/fpls.2016.00794.
- 838 **de Bang, T.C., Lundquist, P.K., Dai, X., Boschiero, C., Zhuang, Z., Pant, P., Torres-Jerez, I.,**
839 **Roy, S., Nogales, J., Veerappan, V., et al.** (2017). Genome-Wide Identification of Medicago
840 Peptides Involved in Macronutrient Responses and Nodulation *Plant Physiology* **175**:1669-1689.
841 10.1104/pp.17.01096.
- 842 **de Carvalho Niebel, F., Lescure, N., Cullimore, J.V., and Gamas, P.** (1998). The *Medicago*
843 *truncatula* *MtAnn1* Gene Encoding an Annexin Is Induced by Nod Factors and During the
844 Symbiotic Interaction with *Rhizobium meliloti*. *Molecular Plant-Microbe Interactions*® **11**:504-
845 513. 10.1094/mpmi.1998.11.6.504.
- 846 **de Zélicourt, A., Diet, A., Marion, J., Laffont, C., Ariel, F., Moison, M., Zahaf, O., Crespi,**
847 **M., Gruber, V., and Frugier, F.** (2012). Dual involvement of a *Medicago truncatula* NAC
848 transcription factor in root abiotic stress response and symbiotic nodule senescence. *The Plant*
849 *journal* **70**:220-230. 10.1111/j.1365-313X.2011.04859.x.
- 850 **Denyer, T., Ma, X., Klesen, S., Scacchi, E., Nieselt, K., and Timmermans, M.C.P.** (2019).
851 Spatiotemporal Developmental Trajectories in the Arabidopsis Root Revealed Using High-
852 Throughput Single-Cell RNA Sequencing. *Developmental cell* **48**:840-852.e845.
853 10.1016/j.devcel.2019.02.022.
- 854 **Di Giacomo, E., Laffont, C., Sciarra, F., Iannelli, M.A., Frugier, F., and Frugis, G.** (2017).
855 KNAT3/4/5-like class 2 KNOX transcription factors are involved in *Medicago truncatula*
856 symbiotic nodule organ development. *New Phytol* **213**:822-837. 10.1111/nph.14146.
- 857 **Dolgikh, E.A., Kusakin, P.G., Kitaeva, A.B., Tsyganova, A.V., Kirienko, A.N., Leppyanen,**
858 **I.V., Dolgikh, A.V., Ilina, E.L., Demchenko, K.N., Tikhonovich, I.A., et al.** (2020). Mutational
859 analysis indicates that abnormalities in rhizobial infection and subsequent plant cell and bacteroid
860 differentiation in pea (*Pisum sativum*) nodules coincide with abnormal cytokinin responses and
861 localization. *Ann Bot* **125**:905-923. 10.1093/aob/mcaa022.

- 862 **Dong, W., Zhu, Y., Chang, H., Wang, C., Yang, J., Shi, J., Gao, J., Yang, W., Lan, L., Wang,**
863 **Y., et al.** (2021). An SHR-SCR module specifies legume cortical cell fate to enable nodulation.
864 *Nature* **589**:586-590. 10.1038/s41586-020-3016-z.
- 865 **Endre, G., Kereszt, A., Kevei, Z., Mihacea, S., Kaló, P., and Kiss, G.B.** (2002). A receptor
866 kinase gene regulating symbiotic nodule development. *Nature* **417**:962-966. 10.1038/nature00842.
- 867 **Farmer, A., Thibivilliers, S., Ryu, K.H., Schiefelbein, J., and Libault, M.** (2021). Single-
868 nucleus RNA and ATAC sequencing reveals the impact of chromatin accessibility on gene
869 expression in *Arabidopsis* roots at the single-cell level. *Mol Plant* **14**:372-383.
870 10.1016/j.molp.2021.01.001.
- 871 **Fendrych, M., Van Hautegeem, T., Van Durme, M., Olvera-Carrillo, Y., Huysmans, M.,**
872 **Karimi, M., Lippens, S., Guérin, Christopher J., Krebs, M., Schumacher, K., et al.** (2014).
873 Programmed Cell Death Controlled by ANAC033/SOMBRERO Determines Root Cap Organ Size
874 in *Arabidopsis*. *Current Biology* **24**:931-940. 10.1016/j.cub.2014.03.025.
- 875 **Fonouni-Farde, C., Kisiala, A., Brault, M., Emery, R.J.N., Diet, A., and Frugier, F.** (2017).
876 DELLA1-Mediated Gibberellin Signaling Regulates Cytokinin-Dependent Symbiotic Nodulation.
877 *Plant physiology* **175**:1795-1806. 10.1104/pp.17.00919.
- 878 **Fonouni-Farde, C., Tan, S., Baudin, M., Brault, M., Wen, J., Mysore, K.S., Niebel, A.,**
879 **Frugier, F., and Diet, A.** (2016). DELLA-mediated gibberellin signalling regulates Nod factor
880 signalling and rhizobial infection. *Nature Communications* **7**:12636. 10.1038/ncomms12636.
- 881 **Franssen, H.J., Xiao, T.T., Kulikova, O., Wan, X., Bisseling, T., Scheres, B., and Heidstra,**
882 **R.** (2015). Root developmental programs shape the *Medicago truncatula* nodule meristem.
883 *Development* **142**:2941-2950. 10.1242/dev.120774.
- 884 **Frugier, F., Poirier, S., Satiat-Jeunemaître, B., Kondorosi, A., and Crespi, M.** (2000). A
885 Krüppel-like zinc finger protein is involved in nitrogen-fixing root nodule organogenesis. *Genes*
886 *& development* **14**:475-482.
- 887 **Gamas, P., Brault, M., Jardinaud, M.F., and Frugier, F.** (2017). Cytokinins in Symbiotic
888 Nodulation: When, Where, What For? *Trends Plant Sci* **22**:792-802.
889 10.1016/j.tplants.2017.06.012.
- 890 **Gao, L.L., Anderson, J.P., Klingler, J.P., Nair, R.M., Edwards, O.R., and Singh, K.B.** (2007).
891 Involvement of the octadecanoid pathway in bluegreen aphid resistance in *Medicago truncatula*.
892 *Mol Plant Microbe Interact* **20**:82-93. 10.1094/mpmi-20-0082.

- 893 **Gaude, N., Bortfeld, S., Duensing, N., Lohse, M., and Krajinski, F.** (2012). Arbuscule-
894 containing and non-colonized cortical cells of mycorrhizal roots undergo extensive and specific
895 reprogramming during arbuscular mycorrhizal development. *Plant J* **69**:510-528. 10.1111/j.1365-
896 313X.2011.04810.x.
- 897 **Gautrat, P., Laffont, C., Frugier, F., and Ruffel, S.** (2021). Nitrogen Systemic Signaling: From
898 Symbiotic Nodulation to Root Acquisition. *Trends Plant Sci* **26**:392-406.
899 10.1016/j.tplants.2020.11.009.
- 900 **Gautrat, P., Mortier, V., Laffont, C., De Keyser, A., Fromentin, J., Frugier, F., and**
901 **Goormachtig, S.** (2019). Unraveling new molecular players involved in the autoregulation of
902 nodulation in *Medicago truncatula*. *Journal of experimental botany* **70**:1407-1417.
903 10.1093/jxb/ery465.
- 904 **Gavrin, A., Kulikova, O., Bisseling, T., and Fedorova, E.E.** (2017). Interface Symbiotic
905 Membrane Formation in Root Nodules of *Medicago truncatula*: the Role of Synaptotagmins
906 MtSyt1, MtSyt2 and MtSyt3. *Frontiers in Plant Science* **8**10.3389/fpls.2017.00201.
- 907 **Gavrin, A., Jansen, V., Ivanov, S., Bisseling, T., and Fedorova, E.** (2015). ARP2/3-Mediated
908 Actin Nucleation Associated With Symbiosome Membrane Is Essential for the Development of
909 Symbiosomes in Infected Cells of *Medicago truncatula* Root Nodules. *Molecular plant-microbe*
910 *interactions : MPMI* **28**:605-614. 10.1094/mpmi-12-14-0402-r.
- 911 **Ge, L., Yu, J., Wang, H., Luth, D., Bai, G., Wang, K., and Chen, R.** (2016). Increasing seed
912 size and quality by manipulating BIG SEEDS1 in legume species. *P Natl Acad Sci USA*
913 **113**:12414-12419. 10.1073/pnas.1611763113.
- 914 **Gleason, C., Chaudhuri, S., Yang, T., Muñoz, A., Poovaiah, B.W., and Oldroyd, G.E.** (2006).
915 Nodulation independent of rhizobia induced by a calcium-activated kinase lacking autoinhibition.
916 *Nature* **441**:1149-1152. 10.1038/nature04812.
- 917 **Gonzalez-Rizzo, S., Crespi, M., and Frugier, F.** (2006). The *Medicago truncatula* CRE1
918 cytokinin receptor regulates lateral root development and early symbiotic interaction with
919 *Sinorhizobium meliloti*. *The Plant cell* **18**:2680-2693. 10.1105/tpc.106.043778.
- 920 **Gough, C., Cottret, L., Lefebvre, B., and Bono, J.-J.** (2018). Evolutionary History of Plant
921 LysM Receptor Proteins Related to Root Endosymbiosis. *Frontiers in Plant Science*
922 **9**10.3389/fpls.2018.00923.

- 923 **Haney, C.H., and Long, S.R.** (2010). Plant flotillins are required for infection by nitrogen-fixing
924 bacteria. *Proc Natl Acad Sci U S A* **107**:478-483. 10.1073/pnas.0910081107.
- 925 **Hao, Y., Hao, S., Andersen-Nissen, E., Mauck, W.M., Zheng, S., Butler, A., Lee, M.J., Wilk,**
926 **A.J., Darby, C., Zager, M., et al.** (2021). Integrated analysis of multimodal single-cell data. *Cell*
927 **184**:3573-3587.e3529. 10.1016/j.cell.2021.04.048.
- 928 **Heidstra, R., Yang, W.C., Yalcin, Y., Peck, S., Emons, A.M., van Kammen, A., and Bisseling,**
929 **T.** (1997). Ethylene provides positional information on cortical cell division but is not involved in
930 Nod factor-induced root hair tip growth in *Rhizobium*-legume interaction. *Development*
931 (Cambridge, England) **124**:1781-1787. 10.1242/dev.124.9.1781.
- 932 **Heo, J.-o., Blob, B., and Helariutta, Y.** (2017). Differentiation of conductive cells: a matter of
933 life and death. *Current Opinion in Plant Biology* **35**:23-29. 10.1016/j.cpb.2016.10.007.
- 934 **Hohnjec, N., Perlick, A.M., Pühler, A., and Küster, H.** (2003). The *Medicago truncatula*
935 Sucrose Synthase Gene *MtSucS1* Is Activated Both in the Infected Region of Root Nodules and in
936 the Cortex of Roots Colonized by Arbuscular Mycorrhizal Fungi. *Molecular Plant-Microbe*
937 *Interactions*® **16**:903-915. 10.1094/mpmi.2003.16.10.903.
- 938 **Huault, E., Laffont, C., Wen, J., Mysore, K.S., Ratet, P., Duc, G., and Frugier, F.** (2014).
939 Local and Systemic Regulation of Plant Root System Architecture and Symbiotic Nodulation by
940 a Receptor-Like Kinase. *PLOS Genetics* **10**:e1004891. 10.1371/journal.pgen.1004891.
- 941 **Huo, X., Schnabel, E., Hughes, K., and Frugoli, J.** (2006). RNAi Phenotypes and the
942 Localization of a Protein::GUS Fusion Imply a Role for *Medicago truncatula* *PIN* Genes in
943 Nodulation. *Journal of plant growth regulation* **25**:156-165. 10.1007/s00344-005-0106-y.
- 944 **Ivanov, S., Fedorova, E.E., Limpens, E., De Mita, S., Genre, A., Bonfante, P., and Bisseling,**
945 **T.** (2012). *Rhizobium*-legume symbiosis shares an exocytotic pathway required for arbuscule
946 formation. *Proceedings of the National Academy of Sciences of the United States of America*
947 **109**:8316-8321. 10.1073/pnas.1200407109.
- 948 **Ivashuta, S., Liu, J., Liu, J., Lohar, D.P., Haridas, S., Bucciarelli, B., VandenBosch, K.A.,**
949 **Vance, C.P., Harrison, M.J., and Gantt, J.S.** (2005). RNA interference identifies a calcium-
950 dependent protein kinase involved in *Medicago truncatula* root development. *The Plant cell*
951 **17**:2911-2921. 10.1105/tpc.105.035394.
- 952 **Jardinaud, M.F., Boivin, S., Rodde, N., Catrice, O., Kisiala, A., Lepage, A., Moreau, S., Roux,**
953 **B., Cottret, L., Sallet, E., et al.** (2016). A Laser Dissection-RNAseq Analysis Highlights the

- 954 Activation of Cytokinin Pathways by Nod Factors in the *Medicago truncatula* Root Epidermis.
955 Plant Physiol **171**:2256-2276. 10.1104/pp.16.00711.
- 956 **Jean-Baptiste, K., McFaline-Figueroa, J.L., Alexandre, C.M., Dorrity, M.W., Saunders, L.,**
957 **Bubb, K.L., Trapnell, C., Fields, S., Queitsch, C., and Cuperus, J.T.** (2019). Dynamics of Gene
958 Expression in Single Root Cells of *Arabidopsis thaliana*. Plant Cell **31**:993-1011.
959 10.1105/tpc.18.00785.
- 960 **Kaló, P., Gleason, C., Edwards, A., Marsh, J., Mitra, R.M., Hirsch, S., Jakab, J., Sims, S.,**
961 **Long, S.R., Rogers, J., et al.** (2005). Nodulation signaling in legumes requires NSP2, a member
962 of the GRAS family of transcriptional regulators. Science **308**:1786-1789.
963 10.1126/science.1110951.
- 964 **Kassaw, T., Nowak, S., Schnabel, E., and Frugoli, J.** (2017). ROOT DETERMINED
965 NODULATION1 Is Required for *M. truncatula* CLE12, But Not CLE13, Peptide Signaling
966 through the SUNN Receptor Kinase Plant Physiology **174**:2445-2456. 10.1104/pp.17.00278.
- 967 **Kim, G.B., Son, S.U., Yu, H.J., and Mun, J.H.** (2019). MtGA2ox10 encoding C20-GA2-oxidase
968 regulates rhizobial infection and nodule development in *Medicago truncatula*. Sci Rep **9**:5952.
969 10.1038/s41598-019-42407-3.
- 970 **Kiss, E., Oláh, B.r., Kaló, P.t., Morales, M., Heckmann, A.B., Borbola, A., Lózsa, A., Kontár,**
971 **K., Middleton, P., Downie, J.A., et al.** (2009). LIN, a Novel Type of U-Box/WD40 Protein,
972 Controls Early Infection by Rhizobia in Legumes. Plant Physiology **151**:1239-1249.
973 10.1104/pp.109.143933.
- 974 **Kumpf, R.P., and Nowack, M.K.** (2015). The root cap: a short story of life and death. Journal of
975 experimental botany **66**:5651-5662. 10.1093/jxb/erv295.
- 976 **Kuppusamy, K.T., Ivashuta, S., Bucciarelli, B., Vance, C.P., Gantt, J.S., and VandenBosch,**
977 **K.A.** (2009). Knockdown of *CELL DIVISION CYCLE16* Reveals an Inverse Relationship between
978 Lateral Root and Nodule Numbers and a Link to Auxin in *Medicago truncatula*. Plant Physiology
979 **151**:1155-1166. 10.1104/pp.109.143024.
- 980 **Laffont, C., De Cuyper, C., Fromentin, J., Mortier, V., De Keyser, A., Verplancke, C.,**
981 **Holsters, M., Goormachtig, S., and Frugier, F.** (2018). MtNRLK1, a CLAVATA1-like leucine-
982 rich repeat receptor-like kinase upregulated during nodulation in *Medicago truncatula*. Scientific
983 Reports **8**:2046. 10.1038/s41598-018-20359-4.

- 984 **Larrainzar, E., Riely, B.K., Kim, S.C., Carrasquilla-Garcia, N., Yu, H.J., Hwang, H.J., Oh,**
985 **M., Kim, G.B., Surendrarao, A.K., Chasman, D., et al.** (2015). Deep Sequencing of the
986 *Medicago truncatula* Root Transcriptome Reveals a Massive and Early Interaction between
987 Nodulation Factor and Ethylene Signals. *Plant Physiol* **169**:233-265. 10.1104/pp.15.00350.
- 988 **Libault, M., Govindarajulu, M., Berg, R.H., Ong, Y.T., Puricelli, K., Taylor, C.G., Xu, D.,**
989 **and Stacey, G.** (2011). A Dual-Targeted Soybean Protein Is Involved in *Bradyrhizobium*
990 *japonicum* Infection of Soybean Root Hair and Cortical Cells. *Molecular Plant-Microbe*
991 *Interactions* **24**:1051-1060. 10.1094/mpmi-12-10-0281.
- 992 **Libault, M., Farmer, A., Brechenmacher, L., Drnevich, J., Langley, R.J., Bilgin, D.D.,**
993 **Radwan, O., Neece, D.J., Clough, S.J., May, G.D., et al.** (2009). Complete Transcriptome of the
994 Soybean Root Hair Cell, a Single-Cell Model, and Its Alteration in Response to *Bradyrhizobium*
995 *japonicum* Infection. *Plant Physiology* **152**:541-552. 10.1104/pp.109.148379.
- 996 **Limpens, E., Ivanov, S., van Esse, W., Voets, G., Fedorova, E., and Bisseling, T.** (2009).
997 *Medicago* N₂-fixing symbiosomes acquire the endocytic identity marker Rab7 but delay the
998 acquisition of vacuolar identity. *The Plant cell* **21**:2811-2828. 10.1105/tpc.108.064410.
- 999 **Lin, J., Roswanjaya, Y.P., Kohlen, W., Stougaard, J., and Reid, D.** (2021). Nitrate restricts
1000 nodule organogenesis through inhibition of cytokinin biosynthesis in *Lotus japonicus*. *Nature*
1001 *Communications* **12**:6544. 10.1038/s41467-021-26820-9.
- 1002 **Liu, C.-W., Breakspear, A., Stacey, N., Findlay, K., Nakashima, J., Ramakrishnan, K., Liu,**
1003 **M., Xie, F., Endre, G., de Carvalho-Niebel, F., et al.** (2019a). A protein complex required for
1004 polar growth of rhizobial infection threads. *Nature Communications* **10**:2848. 10.1038/s41467-
1005 019-10029-y.
- 1006 **Liu, C.-W., Breakspear, A., Guan, D., Cerri, M.R., Jackson, K., Jiang, S., Robson, F.,**
1007 **Radhakrishnan, G.V., Roy, S., Bone, C., et al.** (2019b). NIN Acts as a Network Hub Controlling
1008 a Growth Module Required for Rhizobial Infection. *Plant Physiology* **179**:1704-1722.
1009 10.1104/pp.18.01572.
- 1010 **Liu, J., Deng, J., Zhu, F., Li, Y., Lu, Z., Qin, P., Wang, T., and Dong, J.** (2018). The MtDMI2-
1011 MtPUB2 Negative Feedback Loop Plays a Role in Nodulation Homeostasis *Plant Physiology*
1012 **176**:3003-3026. 10.1104/pp.17.01587.

- 1013 **Liu, Q., Liang, Z., Feng, D., Jiang, S., Wang, Y., Du, Z., Li, R., Hu, G., Zhang, P., Ma, Y., et**
1014 **al.** (2021). Transcriptional landscape of rice roots at the single-cell resolution. *Mol Plant* **14**:384-
1015 394. 10.1016/j.molp.2020.12.014.
- 1016 **Liu, W., Kohlen, W., Lillo, A., Op den Camp, R., Ivanov, S., Hartog, M., Limpens, E., Jamil,**
1017 **M., Smaczniak, C., Kaufmann, K., et al.** (2011). Strigolactone biosynthesis in *Medicago*
1018 *truncatula* and rice requires the symbiotic GRAS-type transcription factors NSP1 and NSP2. *Plant*
1019 *Cell* **23**:3853-3865. 10.1105/tpc.111.089771.
- 1020 **Lohar, D.P., Sharopova, N., Endre, G., Peñuela, S., Samac, D., Town, C., Silverstein, K.A.T.,**
1021 **and VandenBosch, K.A.** (2005). Transcript Analysis of Early Nodulation Events in *Medicago*
1022 *truncatula*. *Plant Physiology* **140**:221-234. 10.1104/pp.105.070326.
- 1023 **Luo, Z., Lin, J.-s., Zhu, Y., Fu, M., Li, X., and Xie, F.** (2021). NLP1 reciprocally regulates
1024 nitrate inhibition of nodulation through SUNN-CRA2 signaling in *Medicago truncatula*. *Plant*
1025 *Communications* **2**:100183. <https://doi.org/10.1016/j.xplc.2021.100183>.
- 1026 **Lyons, E., and Freeling, M.** (2008). How to usefully compare homologous plant genes and
1027 chromosomes as DNA sequences. *Plant J* **53**:661-673. 10.1111/j.1365-313X.2007.03326.x.
- 1028 **Lyons, E., Pedersen, B., Kane, J., Alam, M., Ming, R., Tang, H., Wang, X., Bowers, J.,**
1029 **Paterson, A., Lisch, D., et al.** (2008). Finding and Comparing Syntenic Regions among
1030 *Arabidopsis* and the Outgroups Papaya, Poplar, and Grape: CoGe with Rosids. *Plant Physiology*
1031 **148**:1772-1781. 10.1104/pp.108.124867.
- 1032 **Makabe, S., Yamori, W., Kong, K., Niimi, H., and Nakamura, I.** (2017). Expression of rice
1033 45S rRNA promotes cell proliferation, leading to enhancement of growth in transgenic tobacco.
1034 *Plant Biotechnology* **34**:29-38. 10.5511/plantbiotechnology.17.0216a.
- 1035 **Marino, D., Andrio, E., Danchin, E.G.J., Oger, E., Gucciardo, S., Lambert, A., Puppo, A.,**
1036 **and Pauly, N.** (2011). A *Medicago truncatula* NADPH oxidase is involved in symbiotic nodule
1037 functioning. *The New phytologist* **189**:580-592. 10.1111/j.1469-8137.2010.03509.x.
- 1038 **Mbengue, M., Camut, S., de Carvalho-Niebel, F., Deslandes, L., Froidure, S., Klaus-Heisen,**
1039 **D., Moreau, S., Rivas, S., Timmers, T., Hervé, C., et al.** (2010). The *Medicago truncatula* E3
1040 ubiquitin ligase PUB1 interacts with the LYK3 symbiotic receptor and negatively regulates
1041 infection and nodulation. *The Plant cell* **22**:3474-3488. 10.1105/tpc.110.075861.

- 1042 **Mergaert, P., Kereszt, A., and Kondorosi, E.** (2019). Gene Expression in Nitrogen-Fixing
1043 Symbiotic Nodule Cells in *Medicago truncatula* and Other Nodulating Plants. *The Plant Cell*
1044 **32**:42-68. 10.1105/tpc.19.00494.
- 1045 **Messinese, E., Mun, J.H., Yeun, L.H., Jayaraman, D., Rougé, P., Barre, A., Loughon, G.,**
1046 **Schornack, S., Bono, J.J., Cook, D.R., et al.** (2007). A novel nuclear protein interacts with the
1047 symbiotic DMI3 calcium- and calmodulin-dependent protein kinase of *Medicago truncatula*. *Mol*
1048 *Plant Microbe Interact* **20**:912-921. 10.1094/mpmi-20-8-0912.
- 1049 **Miao, Z., Deng, K., Wang, X., and Zhang, X.** (2018). DEsingle for detecting three types of
1050 differential expression in single-cell RNA-seq data. *Bioinformatics* **34**:3223-3224.
1051 10.1093/bioinformatics/bty332.
- 1052 **Middleton, P.H., Jakab, J., Penmetsa, R.V., Starker, C.G., Doll, J., Kaló, P., Prabhu, R.,**
1053 **Marsh, J.F., Mitra, R.M., Kereszt, A., et al.** (2007). An ERF transcription factor in *Medicago*
1054 *truncatula* that is essential for Nod factor signal transduction. *The Plant cell* **19**:1221-1234.
1055 10.1105/tpc.106.048264.
- 1056 **Mohd-Radzman, N.A., Laffont, C., Ivanovici, A., Patel, N., Reid, D., Stougaard, J., Frugier,**
1057 **F., Imin, N., and Djordjevic, M.A.** (2016). Different Pathways Act Downstream of the CEP
1058 Peptide Receptor CRA2 to Regulate Lateral Root and Nodule Development. *Plant Physiol*
1059 **171**:2536-2548. 10.1104/pp.16.00113.
- 1060 **Montiel, J., Fonseca-García, C., and Quinto, C.** (2018). Phylogeny and Expression of NADPH
1061 Oxidases during Symbiotic Nodule Formation. *Agriculture* **8**:179.
- 1062 **Montiel, J., Arthikala, M.K., Cárdenas, L., and Quinto, C.** (2016). Legume NADPH Oxidases
1063 Have Crucial Roles at Different Stages of Nodulation. *International journal of molecular sciences*
1064 **17**10.3390/ijms17050680.
- 1065 **Müller, L.M., Flokova, K., Schnabel, E., Sun, X., Fei, Z., Frugoli, J., Bouwmeester, H.J., and**
1066 **Harrison, M.J.** (2019). A CLE-SUNN module regulates strigolactone content and fungal
1067 colonization in arbuscular mycorrhiza. *Nat Plants* **5**:933-939. 10.1038/s41477-019-0501-1.
- 1068 **Murray, J.D., Karas, B.J., Sato, S., Tabata, S., Amyot, L., and Szczyglowski, K.** (2007). A
1069 cytokinin perception mutant colonized by *Rhizobium* in the absence of nodule organogenesis.
1070 *Science* **315**:101-104. 10.1126/science.1132514.
- 1071 **Murray, J.D., Muni, R.R., Torres-Jerez, I., Tang, Y., Allen, S., Andriankaja, M., Li, G.,**
1072 **Laxmi, A., Cheng, X., Wen, J., et al.** (2011). Vapyrin, a gene essential for intracellular

- 1073 progression of arbuscular mycorrhizal symbiosis, is also essential for infection by rhizobia in the
1074 nodule symbiosis of *Medicago truncatula*. The Plant journal **65**:244-252. 10.1111/j.1365-
1075 313X.2010.04415.x.
- 1076 **Nguyen, N.N.T., Clua, J., Vetal, P.V., Vuarambon, D.J., De Bellis, D., Pervent, M., Lepetit,**
1077 **M., Udvardi, M., Valentine, A.J., and Poirier, Y.** (2020). PHO1 family members transport
1078 phosphate from infected nodule cells to bacteroids in *Medicago truncatula*. Plant Physiology
1079 **185**:196-209. 10.1093/plphys/kiaa016.
- 1080 **Nutman, P.S.** (1959). Some Observations on Root-Hair Infection by Nodule Bacteria. Journal of
1081 Experimental Botany **10**:250-263. 10.1093/jxb/10.2.250.
- 1082 **Olvera-Carrillo, Y., Van Bel, M., Van Hautegeem, T., Fendrych, M., Huysmans, M.,**
1083 **Simaskova, M., van Durme, M., Buscaill, P., Rivas, S., Coll, N.S., et al.** (2015). A Conserved
1084 Core of Programmed Cell Death Indicator Genes Discriminates Developmentally and
1085 Environmentally Induced Programmed Cell Death in Plants. Plant Physiol **169**:2684-2699.
1086 10.1104/pp.15.00769.
- 1087 **Ouyang, J.F., Kamaraj, U.S., Cao, E.Y., and Rackham, O.J.L.** (2021). ShinyCell: simple and
1088 sharable visualization of single-cell gene expression data. Bioinformatics **37**:3374-3376.
1089 10.1093/bioinformatics/btab209.
- 1090 **Pan, H., Oztas, O., Zhang, X., Wu, X., Stonoha, C., Wang, E., Wang, B., and Wang, D.** (2016).
1091 A symbiotic SNARE protein generated by alternative termination of transcription. Nature plants
1092 **2**:15197. 10.1038/nplants.2015.197.
- 1093 **Pawela, A., Banasiak, J., Biala, W., Martinoia, E., and Jasiński, M.** (2019). MtABCG20 is an
1094 ABA exporter influencing root morphology and seed germination of *Medicago truncatula*. Plant
1095 **J** **98**:511-523. 10.1111/tpj.14234.
- 1096 **Pecrix, Y., Staton, S.E., Sallet, E., Lelandais-Brière, C., Moreau, S., Carrère, S., Blein, T.,**
1097 **Jardinaud, M.-F., Latrassé, D., Zouine, M., et al.** (2018). Whole-genome landscape of
1098 *Medicago truncatula* symbiotic genes. Nat Plants **4**:1017-1025. 10.1038/s41477-018-0286-7.
- 1099 **Penmetsa, R.V., Uribe, P., Anderson, J., Lichtenzveig, J., Gish, J.C., Nam, Y.W., Engstrom,**
1100 **E., Xu, K., Sckisel, G., Pereira, M., et al.** (2008). The *Medicago truncatula* ortholog of
1101 Arabidopsis *EIN2*, *sickle*, is a negative regulator of symbiotic and pathogenic microbial
1102 associations. Plant J **55**:580-595. 10.1111/j.1365-313X.2008.03531.x.

- 1103 **Pingault, L., Zogli, P., Brooks, J., and Libault, M.** (2018). Enhancing Phenotyping and
1104 Molecular Analysis of Plant Root System Using Ultrasound Aeroponic Technology. *Curr Protoc*
1105 *Plant Biol* **3**:e20078. 10.1002/cppb.20078.
- 1106 **Plet, J., Wasson, A., Ariel, F., Le Signor, C., Baker, D., Mathesius, U., Crespi, M., and**
1107 **Frugier, F.** (2011). MtCRE1-dependent cytokinin signaling integrates bacterial and plant cues to
1108 coordinate symbiotic nodule organogenesis in *Medicago truncatula*. *Plant J* **65**:622-633.
1109 10.1111/j.1365-313X.2010.04447.x.
- 1110 **Ponnala, L., Wang, Y., Sun, Q., and van Wijk, K.J.** (2014). Correlation of mRNA and protein
1111 abundance in the developing maize leaf. *The Plant Journal* **78**:424-440. 10.1111/tpj.12482.
- 1112 **Qiao, Z., Pingault, L., Zogli, P., Langevin, M., Rech, N., Farmer, A., and Libault, M.** (2017).
1113 A comparative genomic and transcriptomic analysis at the level of isolated root hair cells reveals
1114 new conserved root hair regulatory elements. *Plant Mol Biol* **94**:641-655. 10.1007/s11103-017-
1115 0630-8.
- 1116 **Riely, B.K., He, H., Venkateshwaran, M., Sarma, B., Schraiber, J., Ané, J.M., and Cook,**
1117 **D.R.** (2011). Identification of legume *RopGEF* gene families and characterization of a *Medicago*
1118 *truncatula* *RopGEF* mediating polar growth of root hairs. *The Plant journal* **65**:230-243.
1119 10.1111/j.1365-313X.2010.04414.x.
- 1120 **Roy, S., Liu, W., Nandety, R.S., Crook, A., Mysore, K.S., Pislariu, C.I., Frugoli, J., Dickstein,**
1121 **R., and Udvardi, M.K.** (2019). Celebrating 20 Years of Genetic Discoveries in Legume
1122 Nodulation and Symbiotic Nitrogen Fixation. *The Plant Cell* **32**:15-41. 10.1105/tpc.19.00279.
- 1123 **Roy, S., Robson, F., Lilley, J., Liu, C.W., Cheng, X., Wen, J., Walker, S., Sun, J., Cousins,**
1124 **D., Bone, C., et al.** (2017). *MtLAX2*, a Functional Homologue of the Arabidopsis Auxin Influx
1125 Transporter AUX1, Is Required for Nodule Organogenesis. *Plant Physiol* **174**:326-338.
1126 10.1104/pp.16.01473.
- 1127 **Ryu, K.H., Huang, L., Kang, H.M., and Schiefelbein, J.** (2019). Single-Cell RNA Sequencing
1128 Resolves Molecular Relationships Among Individual Plant Cells. *Plant Physiol* **179**:1444-1456.
1129 10.1104/pp.18.01482.
- 1130 **Schauser, L., Roussis, A., Stiller, J., and Stougaard, J.** (1999). A plant regulator controlling
1131 development of symbiotic root nodules. *Nature* **402**:191-195. 10.1038/46058.
- 1132 **Schiessl, K., Lilley, J.L.S., Lee, T., Tamvakis, I., Kohlen, W., Bailey, P.C., Thomas, A.,**
1133 **Luptak, J., Ramakrishnan, K., Carpenter, M.D., et al.** (2019). NODULE INCEPTION Recruits

1134 the Lateral Root Developmental Program for Symbiotic Nodule Organogenesis in *Medicago*
1135 *truncatula*. *Current biology* : CB **29**:3657-3668.e3655. 10.1016/j.cub.2019.09.005.

1136 **Schnabel, E., Karve, A., Kassaw, T., Mukherjee, A., Zhou, X., Hall, T., and Frugoli, J.** (2012).
1137 The *M. truncatula* *SUNN* gene is expressed in vascular tissue, similarly to *RDNI*, consistent with
1138 the role of these nodulation regulation genes in long distance signaling. *Plant Signal Behav* **7**:4-6.
1139 10.4161/psb.7.1.18491.

1140 **Schnabel, E.L., Kassaw, T.K., Smith, L.S., Marsh, J.F., Oldroyd, G.E., Long, S.R., and**
1141 **Frugoli, J.A.** (2011). The *ROOT DETERMINED NODULATION1* gene regulates nodule number
1142 in roots of *Medicago truncatula* and defines a highly conserved, uncharacterized plant gene family.
1143 *Plant Physiol* **157**:328-340. 10.1104/pp.111.178756.

1144 **Schwacke, R., Ponce-Soto, G.Y., Krause, K., Bolger, A.M., Arsova, B., Hallab, A., Gruden,**
1145 **K., Stitt, M., Bolger, M.E., and Usadel, B.** (2019). MapMan4: A Refined Protein Classification
1146 and Annotation Framework Applicable to Multi-Omics Data Analysis. *Mol Plant* **12**:879-892.
1147 10.1016/j.molp.2019.01.003.

1148 **Shen, C., Yue, R., Sun, T., Zhang, L., Xu, L., Tie, S., Wang, H., and Yang, Y.** (2015). Genome-
1149 wide identification and expression analysis of auxin response factor gene family in *Medicago*
1150 *truncatula*. *Frontiers in plant science* **6**:73-73. 10.3389/fpls.2015.00073.

1151 **Shen, D., Kulikova, O., Guhl, K., Franssen, H., Kohlen, W., Bisseling, T., and Geurts, R.**
1152 (2019). The *Medicago truncatula* nodule identity gene *MtNOOT1* is required for coordinated
1153 apical-basal development of the root. *BMC Plant Biol* **19**:571. 10.1186/s12870-019-2194-z.

1154 **Shulse, C.N., Cole, B.J., Ciobanu, D., Lin, J., Yoshinaga, Y., Gouran, M., Turco, G.M., Zhu,**
1155 **Y., O'Malley, R.C., Brady, S.M., et al.** (2019). High-Throughput Single-Cell Transcriptome
1156 Profiling of Plant Cell Types. *Cell Reports* **27**:2241-2247.e2244. 10.1016/j.celrep.2019.04.054.

1157 **Si, Z., Yang, Q., Liang, R., Chen, L., Chen, D., and Li, Y.** (2019). Digalactosyldiacylglycerol
1158 Synthase Gene *MtDGD1* Plays an Essential Role in Nodule Development and Nitrogen Fixation.
1159 *Mol Plant Microbe Interact* **32**:1196-1209. 10.1094/mpmi-11-18-0322-r.

1160 **Sinharoy, S., Torres-Jerez, I., Bandyopadhyay, K., Kereszt, A., Pislariu, C.I., Nakashima, J.,**
1161 **Benedito, V.A., Kondorosi, E., and Udvardi, M.K.** (2013). The C2H2 transcription factor
1162 regulator of symbiosome differentiation represses transcription of the secretory pathway gene
1163 *VAMP721a* and promotes symbiosome development in *Medicago truncatula*. *The Plant cell*
1164 **25**:3584-3601. 10.1105/tpc.113.114017.

- 1165 **Sinharoy, S., Liu, C., Breakspear, A., Guan, D., Shailes, S., Nakashima, J., Zhang, S., Wen,**
1166 **J., Torres-Jerez, I., Oldroyd, G., et al.** (2016). A *Medicago truncatula* Cystathionine- β -
1167 Synthase-like Domain-Containing Protein Is Required for Rhizobial Infection and Symbiotic
1168 Nitrogen Fixation. *Plant Physiol* **170**:2204-2217. 10.1104/pp.15.01853.
- 1169 **Smit, P., Raedts, J., Portyanko, V., Debellé, F., Gough, C., Bisseling, T., and Geurts, R.**
1170 (2005). NSP1 of the GRAS protein family is essential for rhizobial Nod factor-induced
1171 transcription. *Science* **308**:1789-1791. 10.1126/science.1111025.
- 1172 **Smit, P., Limpens, E., Geurts, R., Fedorova, E., Dolgikh, E., Gough, C., and Bisseling, T.**
1173 (2007). *Medicago* LYK3, an entry receptor in rhizobial nodulation factor signaling. *Plant Physiol*
1174 **145**:183-191. 10.1104/pp.107.100495.
- 1175 **Soyano, T., Shimoda, Y., Kawaguchi, M., and Hayashi, M.** (2019). A shared gene drives lateral
1176 root development and root nodule symbiosis pathways in *Lotus*. *Science* **366**:1021-1023.
1177 10.1126/science.aax2153.
- 1178 **Suzaki, T., Kim, C.S., Takeda, N., Szczyglowski, K., and Kawaguchi, M.** (2013). TRICOT
1179 encodes an AMP1-related carboxypeptidase that regulates root nodule development and shoot
1180 apical meristem maintenance in *Lotus japonicus*. *Development (Cambridge, England)* **140**:353-
1181 361. 10.1242/dev.089631.
- 1182 **Tan, S., Debellé, F., Gamas, P., Frugier, F., and Brault, M.** (2019). Diversification of cytokinin
1183 phosphotransfer signaling genes in *Medicago truncatula* and other legume genomes. *BMC*
1184 *Genomics* **20**:373. 10.1186/s12864-019-5724-z.
- 1185 **Tavormina, P., De Coninck, B., Nikonorova, N., De Smet, I., and Cammue, B.P.A.** (2015).
1186 The Plant Peptidome: An Expanding Repertoire of Structural Features and Biological Functions.
1187 *The Plant Cell* **27**:2095-2118. 10.1105/tpc.15.00440.
- 1188 **Tellström, V., Usadel, B.r., Thimm, O., Stitt, M., Küster, H., and Niehaus, K.** (2007). The
1189 Lipopolysaccharide of *Sinorhizobium meliloti* Suppresses Defense-Associated Gene Expression
1190 in Cell Cultures of the Host Plant *Medicago truncatula*. *Plant Physiology* **143**:825-837.
1191 10.1104/pp.106.090985.
- 1192 **Thibivilliers, S., Anderson, D., and Libault, M.** (2020). Isolation of Plant Root Nuclei for Single
1193 Cell RNA Sequencing. *Current Protocols in Plant Biology* **5**:e20120.
1194 <https://doi.org/10.1002/cppb.20120>.

- 1195 **Thimm, O., Bläsing, O., Gibon, Y., Nagel, A., Meyer, S., Krüger, P., Selbig, J., Müller, L.A.,**
1196 **Rhee, S.Y., and Stitt, M.** (2004). MAPMAN: a user-driven tool to display genomics data sets
1197 onto diagrams of metabolic pathways and other biological processes. *Plant J* **37**:914-939.
1198 10.1111/j.1365-313x.2004.02016.x.
- 1199 **Tian, Y., Liu, W., Cai, J., Zhang, L.Y., Wong, K.B., Feddermann, N., Boller, T., Xie, Z.P.,**
1200 **and Staehelin, C.** (2013). The nodulation factor hydrolase of *Medicago truncatula*:
1201 characterization of an enzyme specifically cleaving rhizobial nodulation signals. *Plant Physiol*
1202 **163**:1179-1190. 10.1104/pp.113.223966.
- 1203 **Turco, G.M., Rodriguez-Medina, J., Siebert, S., Han, D., Valderrama-Gómez, M., Vahldick,**
1204 **H., Shulse, C.N., Cole, B.J., Juliano, C.E., Dickel, D.E., et al.** (2019). Molecular Mechanisms
1205 Driving Switch Behavior in Xylem Cell Differentiation. *Cell Rep* **28**:342-351.e344.
1206 10.1016/j.celrep.2019.06.041.
- 1207 **Van de Velde, W., Zehirov, G., Szatmari, A., Debreczeny, M., Ishihara, H., Kevei, Z., Farkas,**
1208 **A., Mikulass, K., Nagy, A., Tiricz, H., et al.** (2010). Plant peptides govern terminal differentiation
1209 of bacteria in symbiosis. *Science* **327**:1122-1126. 10.1126/science.1184057.
- 1210 **van Zeijl, A., Op den Camp, Rik H.M., Deinum, Eva E., Charnikhova, T., Franssen, H.,**
1211 **Op den Camp, Huub J.M., Bouwmeester, H., Kohlen, W., Bisseling, T., and Geurts, R.**
1212 (2015). Rhizobium Lipo-chitooligosaccharide Signaling Triggers Accumulation of Cytokinins in
1213 *Medicago truncatula* Roots. *Molecular Plant* **8**:1213-1226. 10.1016/j.molp.2015.03.010.
- 1214 **Venkateshwaran, M., Cosme, A., Han, L., Banba, M., Satyshur, K.A., Schleiff, E., Parniske,**
1215 **M., Imaizumi-Anraku, H., and Ané, J.-M.** (2012). The Recent Evolution of a Symbiotic Ion
1216 Channel in the Legume Family Altered Ion Conductance and Improved Functionality in Calcium
1217 Signaling *The Plant cell* **24**:2528-2545. 10.1105/tpc.112.098475.
- 1218 **Verdier, J., Lalanne, D., Pelletier, S., Torres-Jerez, I., Righetti, K., Bandyopadhyay, K.,**
1219 **Leprince, O., Chatelain, E., Vu, B.L., Gouzy, J., et al.** (2013). A Regulatory Network-Based
1220 Approach Dissects Late Maturation Processes Related to the Acquisition of Desiccation Tolerance
1221 and Longevity of *Medicago truncatula* Seeds. *Plant Physiology* **163**:757-774.
1222 10.1104/pp.113.222380.
- 1223 **Vernié, T., Moreau, S., de Billy, F., Plet, J., Combier, J.P., Rogers, C., Oldroyd, G., Frugier,**
1224 **F., Niebel, A., and Gamas, P.** (2008). EFD Is an ERF transcription factor involved in the control

- 1225 of nodule number and differentiation in *Medicago truncatula*. The Plant cell **20**:2696-2713.
1226 10.1105/tpc.108.059857.
- 1227 **Wang, D., Griffitts, J., Starker, C., Fedorova, E., Limpens, E., Ivanov, S., Bisseling, T., and**
1228 **Long, S.** (2010). A nodule-specific protein secretory pathway required for nitrogen-fixing
1229 symbiosis. *Science* **327**:1126-1129. 10.1126/science.1184096.
- 1230 **Wang, J., Hou, Q., Li, P., Yang, L., Sun, X., Benedito, V.A., Wen, J., Chen, B., Mysore, K.S.,**
1231 **and Zhao, J.** (2017). Diverse functions of multidrug and toxin extrusion (MATE) transporters in
1232 citric acid efflux and metal homeostasis in *Medicago truncatula*. *The Plant Journal* **90**:79-95.
1233 <https://doi.org/10.1111/tpj.13471>.
- 1234 **Wang, T., Li, B., Nelson, C.E., and Nabavi, S.** (2019). Comparative analysis of differential gene
1235 expression analysis tools for single-cell RNA sequencing data. *BMC Bioinformatics* **20**:40.
1236 10.1186/s12859-019-2599-6.
- 1237 **Wang, X., Wei, C., He, F., and Yang, Q.** (2022). MtPT5 phosphate transporter is involved in leaf
1238 growth and phosphate accumulation of *Medicago truncatula*. *Front Plant Sci* **13**:1005895.
1239 10.3389/fpls.2022.1005895.
- 1240 **Xiao, T.T., Schilderink, S., Moling, S., Deinum, E.E., Kondorosi, E., Franssen, H., Kulikova,**
1241 **O., Niebel, A., and Bisseling, T.** (2014). Fate map of *Medicago truncatula* root nodules.
1242 *Development* **141**:3517-3528. 10.1242/dev.110775.
- 1243 **Xie, F., Murray, J.D., Kim, J., Heckmann, A.B., Edwards, A., Oldroyd, G.E.D., and Downie,**
1244 **J.A.** (2012). Legume pectate lyase required for root infection by rhizobia. *P Natl Acad Sci USA*
1245 **109**:633-638. 10.1073/pnas.1113992109.
- 1246 **Yoon, H.J., Hossain, M.S., Held, M., Hou, H., Kehl, M., Tromas, A., Sato, S., Tabata, S.,**
1247 **Andersen, S.U., Stougaard, J., et al.** (2014). *Lotus japonicus* *SUNERGOS1* encodes a predicted
1248 subunit A of a DNA topoisomerase VI that is required for nodule differentiation and
1249 accommodation of rhizobial infection. *The Plant journal* **78**:811-821. 10.1111/tpj.12520.
- 1250 **Young, M.D., and Behjati, S.** (2020). SoupX removes ambient RNA contamination from droplet-
1251 based single-cell RNA sequencing data. *Gigascience* **9**ARTN 10; 10.1093/gigascience/giaa151.
- 1252 **Zeng, L., Zhang, N., Zhang, Q., Endress, P.K., Huang, J., and Ma, H.** (2017). Resolution of
1253 deep eudicot phylogeny and their temporal diversification using nuclear genes from transcriptomic
1254 and genomic datasets. *New Phytologist* **214**:1338-1354. 10.1111/nph.14503.

1255 **Zhang, T.-Q., Xu, Z.-G., Shang, G.-D., and Wang, J.-W.** (2019). A Single-Cell RNA
1256 Sequencing Profiles the Developmental Landscape of Arabidopsis Root. *Molecular Plant* **12**:648-
1257 660. 10.1016/j.molp.2019.04.004.

1258 **Zhang, T.-Q., Chen, Y., Liu, Y., Lin, W.-H., and Wang, J.-W.** (2021). Single-cell transcriptome
1259 atlas and chromatin accessibility landscape reveal differentiation trajectories in the rice root.
1260 *Nature Communications* **12**:2053. 10.1038/s41467-021-22352-4.

1261

1262 **Figure legends**

1263 **Figure 1. Single-nuclei RNA-seq of the *M. truncatula* roots reveals 25 different root**
1264 **clusters. A.** UMAP clustering of *M. truncatula* / *E. meliloti*- and mock-inoculated root nuclei
1265 according to their transcriptomic profiles. While the overall topography of these two UMAPs is
1266 well conserved, subtle differences are observed (e.g., highlighted in red for cluster #2). **B.**
1267 Percentage of *E. meliloti* (dash bars) and mock-inoculated (solid bars) nuclei allocated in the 25
1268 clusters composing the *M. truncatula* root UMAP.

1269

1270 **Figure 2. Functional annotation of the 25 *M. truncatula* root clusters. A.** UMAP clustering
1271 and functional annotation of the Medicago root cell-types clusters based on the expression of
1272 Medicago marker genes and of genes orthologous to Arabidopsis root marker genes. **B.**
1273 Normalized expression levels of cell-type marker genes functionally characterized in Medicago
1274 (detailed in Supplemental Table 2), or orthologous to Arabidopsis root cell-type-specific marker
1275 genes (detailed in Supplemental Table 4) across the 25 Medicago root clusters, shown on the y-
1276 axis. The percentage of nuclei expressing the gene of interest (circle size), and the mean
1277 expression (circle color) of genes, are shown for each sub-panel.

1278

1279 **Figure 3. Comparative transcriptomic analysis of the *M. truncatula* and *A. thaliana* root cell**
1280 **clusters. A.** Functional annotation of Arabidopsis root nuclei clusters based on the expression
1281 profile of cell-type marker genes defined from (Farmer *et al.*, 2021). **B.** Pairwise correlations of
1282 Arabidopsis (*x*-axis) and Medicago (*y*-axis) root cell clusters. Only correlation numbers greater
1283 than 0.4 (black numbers) or 0.5 (white numbers) are shown in the heatmap. EC: Epidermal cells;
1284 CC: Cortical cells; SCN: Stem cell niche; EC: Endodermal cells; SC: Stele cells.

1285

1286 **Figure 4. Differential expression of the *M. truncatula* genes in response to *E. meliloti***
 1287 **inoculation across the 25 root cell clusters. A.** The transcriptional response of Medicago root
 1288 cells to *E. meliloti* inoculation differs between cell-type clusters. The number of up- and down-
 1289 regulated genes are highlighted in green and red bars, respectively. The dashed bar reflects the
 1290 500 DEGs thresholds. **B** and **C.** Comparison of the number of DEGs between the cortical cell
 1291 clusters #7 and 11 (**B**) and between the endodermal cell clusters #15, 16, and 18 (**C**). EC:
 1292 Epidermal cells; CC: Cortical cells; SCN: Stem cell niche; EC: Endodermal cells; SC: Stele
 1293 cells.

1294

1295 **Figure 5. Summary of the *M. truncatula* root cell-type specific transcriptional response to**
 1296 **rhizobial inoculation.** Selected genes previously known as related to nodulation and hormonal
 1297 pathways and identified as differentially expressed in the clusters showing more than 500 DEGs
 1298 are listed. Besides the expected induced expression pattern of numerous nodulation-related genes
 1299 such as in the root hair cells cluster #2, more unexpected expression profiles were also highlighted
 1300 notably for some late nodulation genes, and for repressed early nodulation and hormone-related
 1301 genes in cortical and endodermal clusters #7 and 15-18. Genes are listed in the following
 1302 categories: rhizobial infection-related, Nod factor (NF) signaling, other nodulation stages,
 1303 hormones, signaling peptides. Upward arrows indicate gene inductions by rhizobia, and downward
 1304 arrows, repressions.

1305

1306 **Figure 6. Cell-type enrichment of known *M. truncatula* nodulation and cytokinin signaling**
 1307 **genes. A-E.** Normalized expression levels of Medicago nodulation-related genes specifically
 1308 expressed/enriched in the epidermal (**A**), cortical (**B**), endodermal (**C**), and steles cells (**D**), as well
 1309 as of Medicago cytokinin-signaling-related genes (**E**). The 25 Medicago root clusters identified
 1310 are shown on the *x*-axis. The percentage of nuclei expressing the gene of interest (circle size), and
 1311 the mean expression (circle color) of genes, are shown for each sub-panel. M = mock-inoculated
 1312 condition; I: rhizobia-inoculated condition.

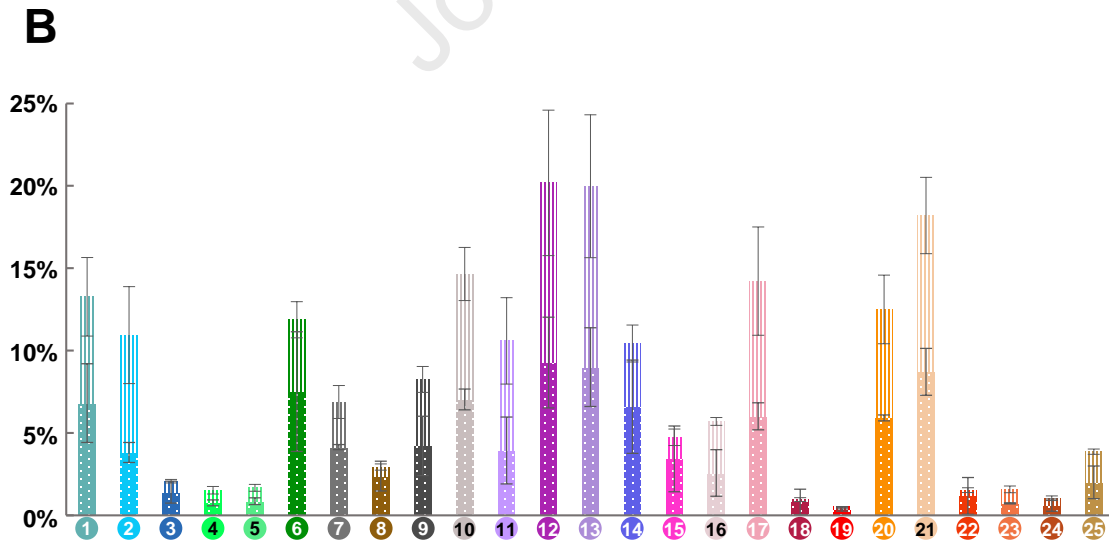
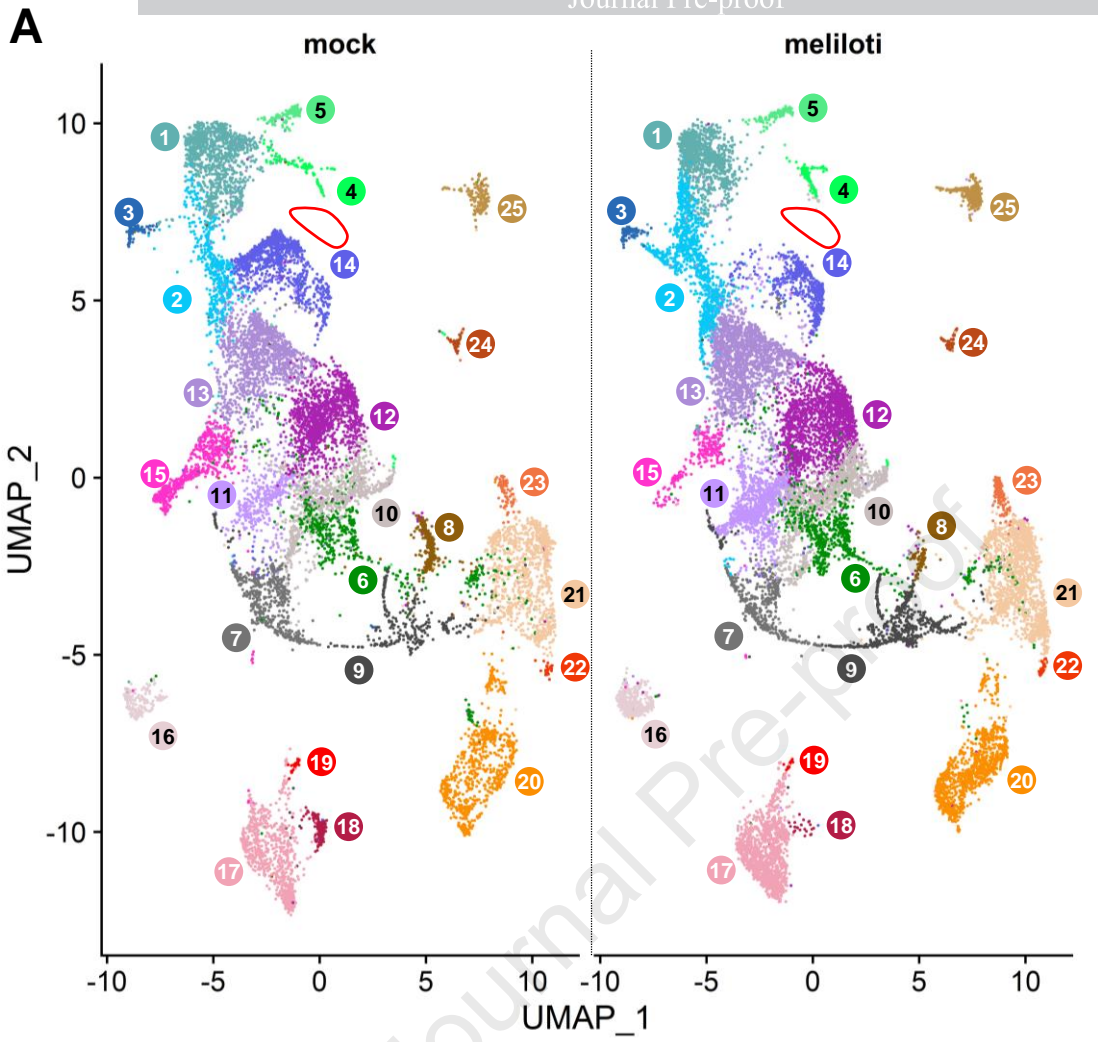
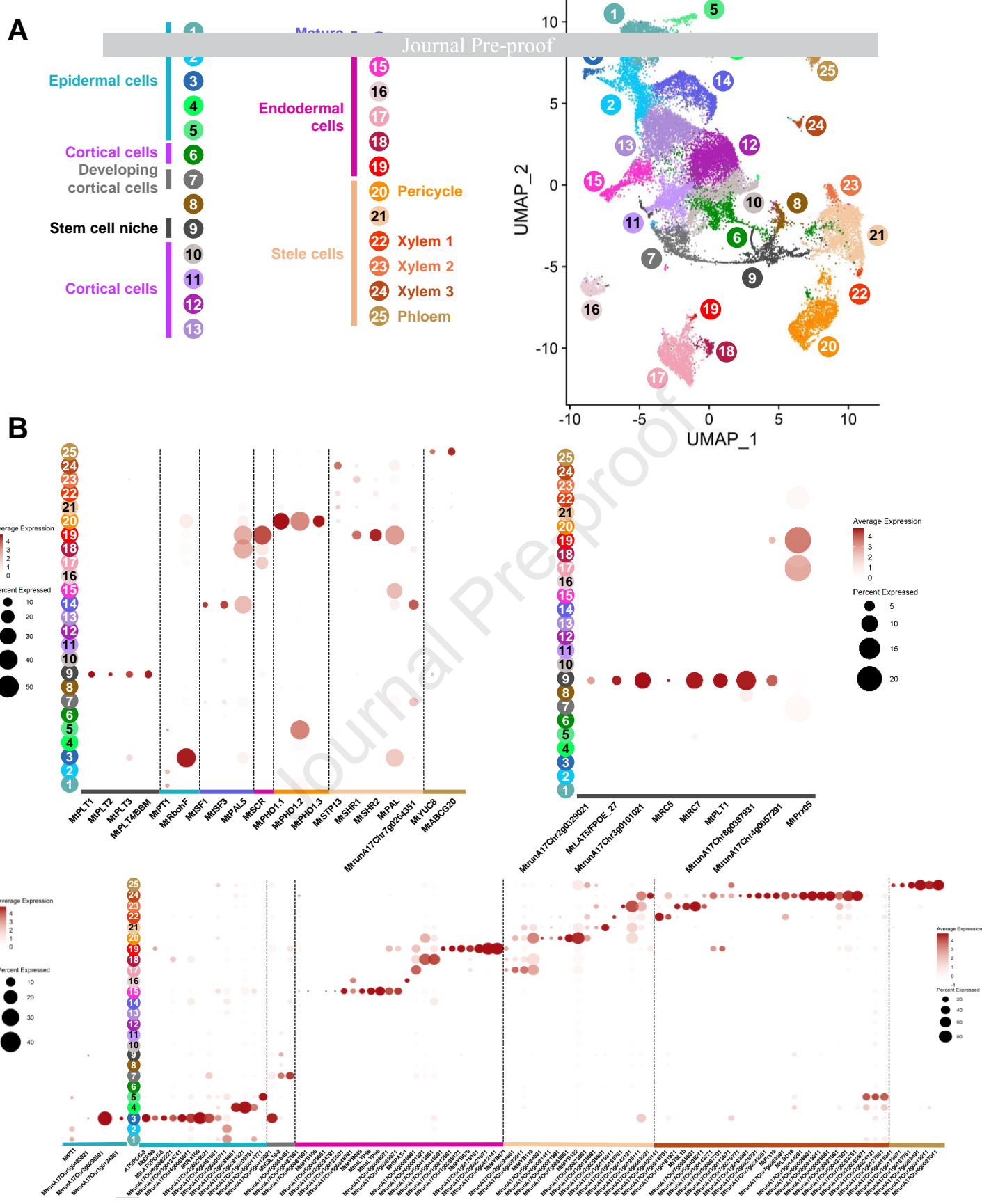
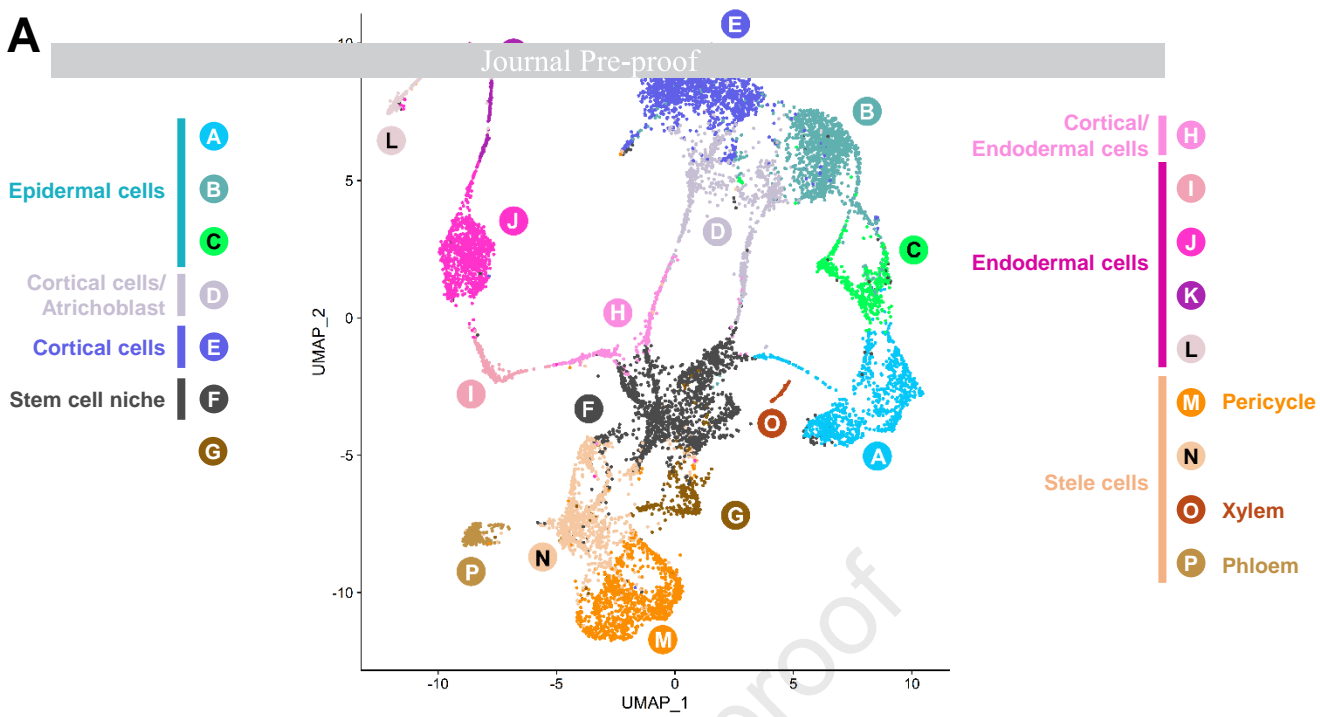


Figure 1.



A



B

Arabidopsis thaliana root

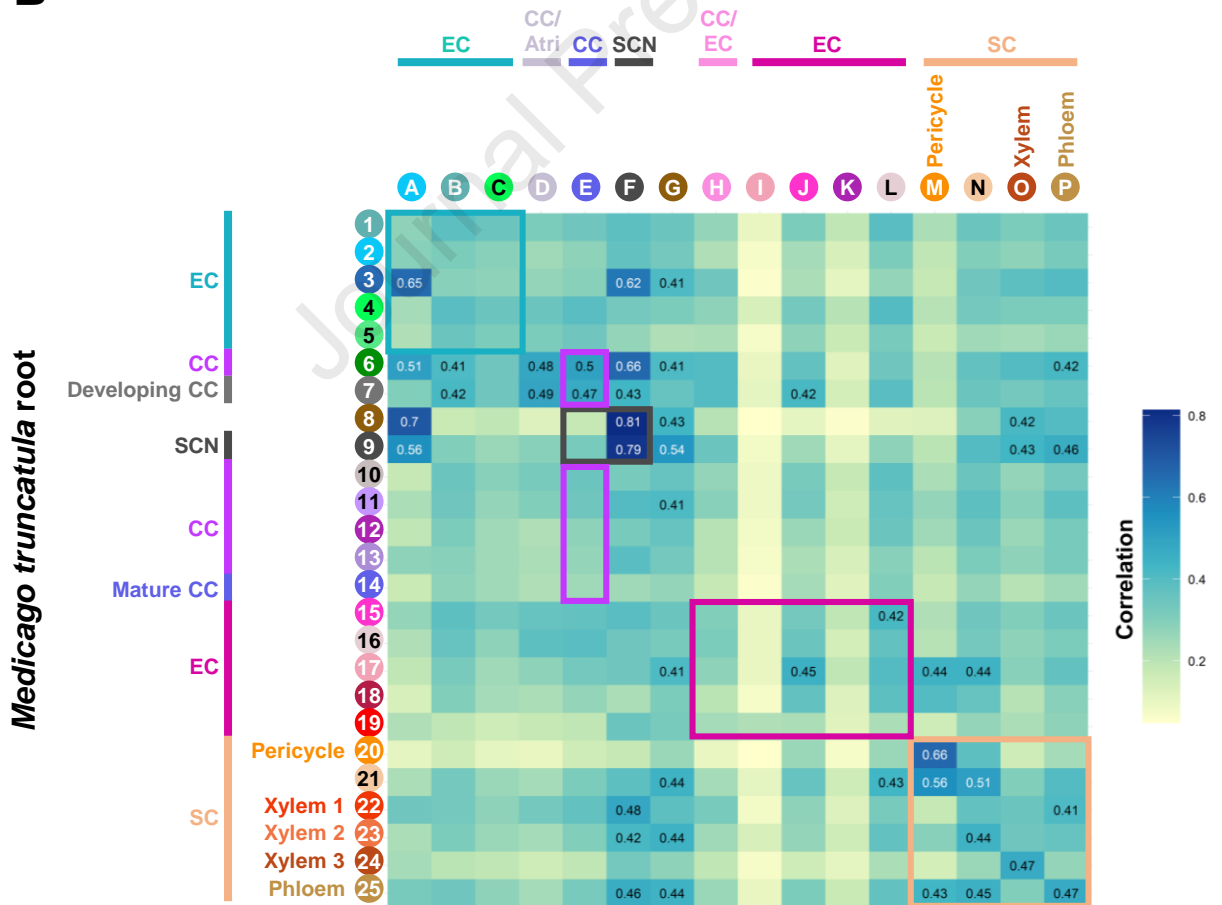
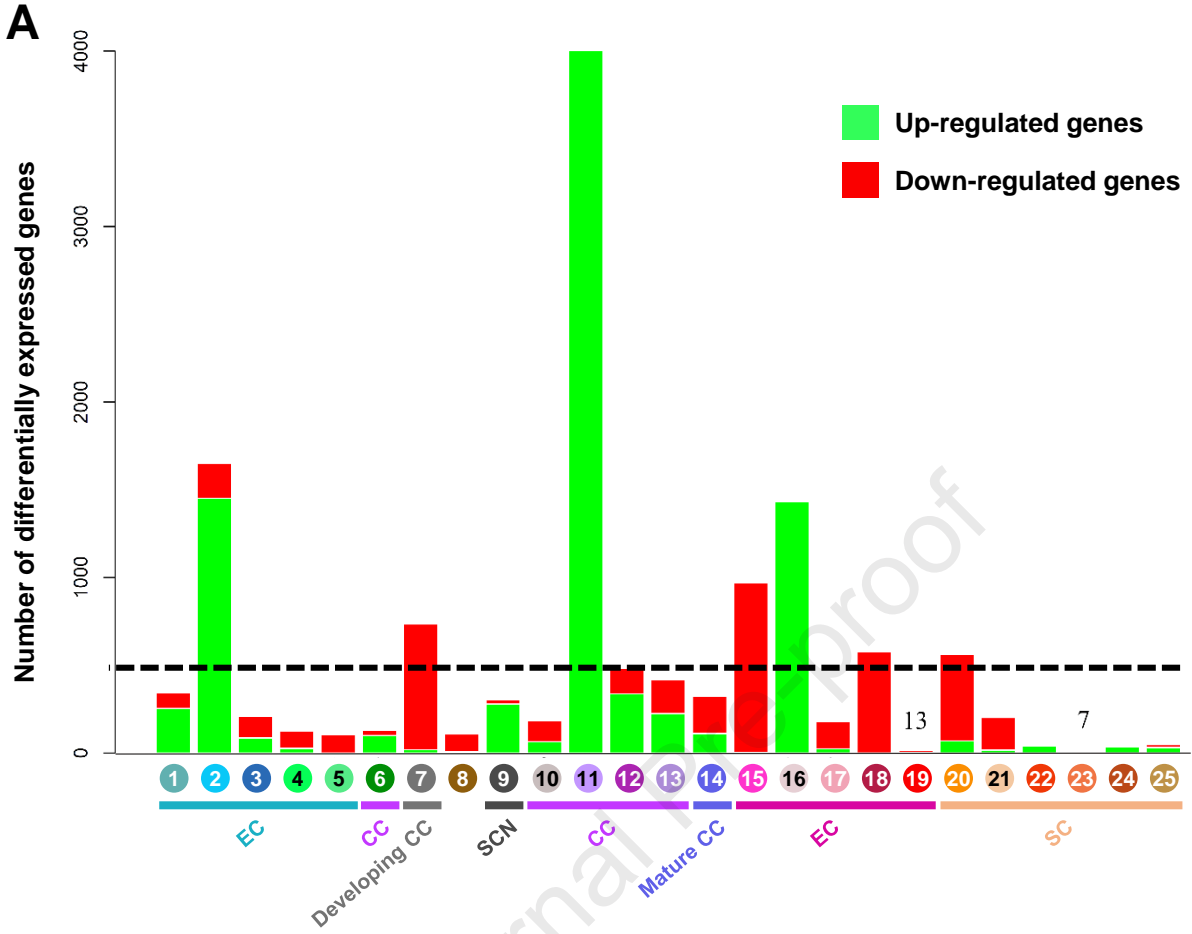
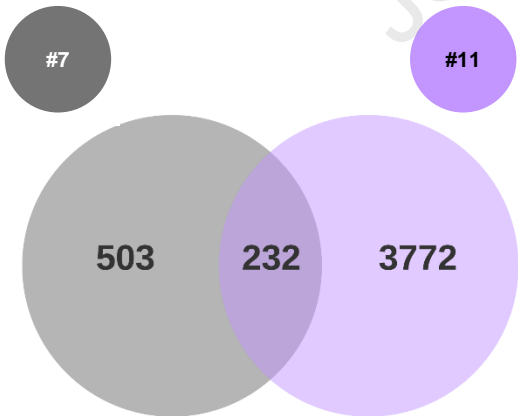


Figure 3.



B



C

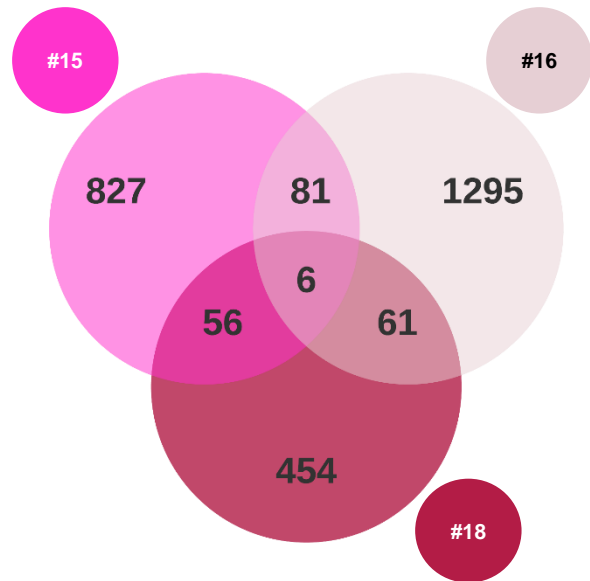


Figure 4.

CLUSTER #4

↑ **Infection-related:** *MtRbohA*, *MtRbohB*, *MtLIN*
 ↑ **NF signaling:** *MtPUB2*, *MtDMI1*, *MtDMI3*, *MtERN2*
 ↑ **Other stages:** *MtSHR1*, *MtKNOX4*, *MtKNOX9*, *MtNOOT1*, *MtCCS52a*, *MtNAC969*
 ↑ **Hormones:** cytokinin (*MtCHK1/MtCRE1*, *MtHPT3*, *MtRRB5*, *MtRRB8*, *MtRRA5*); auxin (*MtARF10*, *MtARF13*, *MtARF24*); gibberellin (*MtDELLA2*); ethylene (*MtETR1*, *MtEIN3*); jasmonic acid (*MtLOX3*, *MtLOX6*); strigolactone (*MtMAX2b*)
 ↑ **Signaling peptides:** *MtRTF/DVL11*

MtVVPY, *MtAnn1*, *MtNMN1*
 ↑ **NF signaling:** *MtNHF1*, *MtLYK10*, *MtPUB1*, *MtIPD3*, *MtDMI1*, *MtDMI2*, *MtDMI3*, *MtNSP1*, *MtNSP2*, *MtERN1*, *MtERN2*, *MtNIN*.
 ↑ **Other stages:** *MtKNOX3*, *MtKNOX5*, *MtDNF2*, *MtNCR112*
 ↑ **Hormones:** cytokinin (*MtIPT1*, *CYP735A1*-like, *MtHPT1*, *MtRRB6*, *MtRRA2*, *MtRRA5*); gibberellin (*MtGA2ox10*, *MtGA3ox1*, *MtDELLA2*); jasmonic acid (*MtLOX6*, *MtJAZ3*); auxin (*MtARF10*); abscisic acid (*MtABI5*); strigolactone (*MtD27*, *MtMAX1a*); ethylene (*MtETR4*); brassinosteroid (*MtBAK1*)
 ↓ **NF signaling/infection:** *MtPUB2*
 ↓ **Signaling peptides:** *MtPIP1*, *MtIDA20*, *MtIDA31*, *MtIDA35*

CLUSTER #7

↓ **NF signaling/infection:** *MtCASTOR*
 ↓ **Hormones:** cytokinin (*MtRRA4*, *MtRRA9*), gibberellin (*MtDELLA1*), abscisic acid (*MtABI5*)

CLUSTER #16

↑ **NF signaling/infection:** *MtCASTOR*
 ↑ **Hormones:** cytokinin (*MtRRB9*); gibberellin (*MtDELLA1*, *MtDELLA2*); auxin (*MtARF2*, *MtARF8*); ethylene (*MtEIN3*); brassinosteroid (*MtBAK1*)

CLUSTER #18

↓ **NF signaling:** *MtDMI3*
 ↓ **Other stages:** *MtZPT2-1*, *MtZPT2-2*.
 ↓ **Hormones:** cytokinin (*MtRRB24*)
 ↓ **Signaling peptides:** *MtPIP1*

CLUSTER #20

↑ **Other stages:** *MtNRLK1*
 ↓ **Other stages:** *MtRbohG*, *MtENOD40*, *MtZPT2-1*, *MtZPT2-2*, *MtKNOX9*
 ↓ **Hormones:** cytokinin (*MtRRB5*); auxin (*MtYUC8*, *MtSERK*); ethylene (*MtEBF1*)
 ↓ **Signaling peptides:** *MtIDA33*

CLUSTER #15

↓ **Infection-related:** *MtLIN*, *MtPUB2*, *MtENODL13*
 ↓ **NF signaling:** *MtDMI2*
 ↓ **Other stages:** *MtZPT2-1*, *MtDNF2*
 ↓ **Hormones:** cytokinin (*MtCHK1/MtCRE1*, *MtRRA2*)

Figure 5.

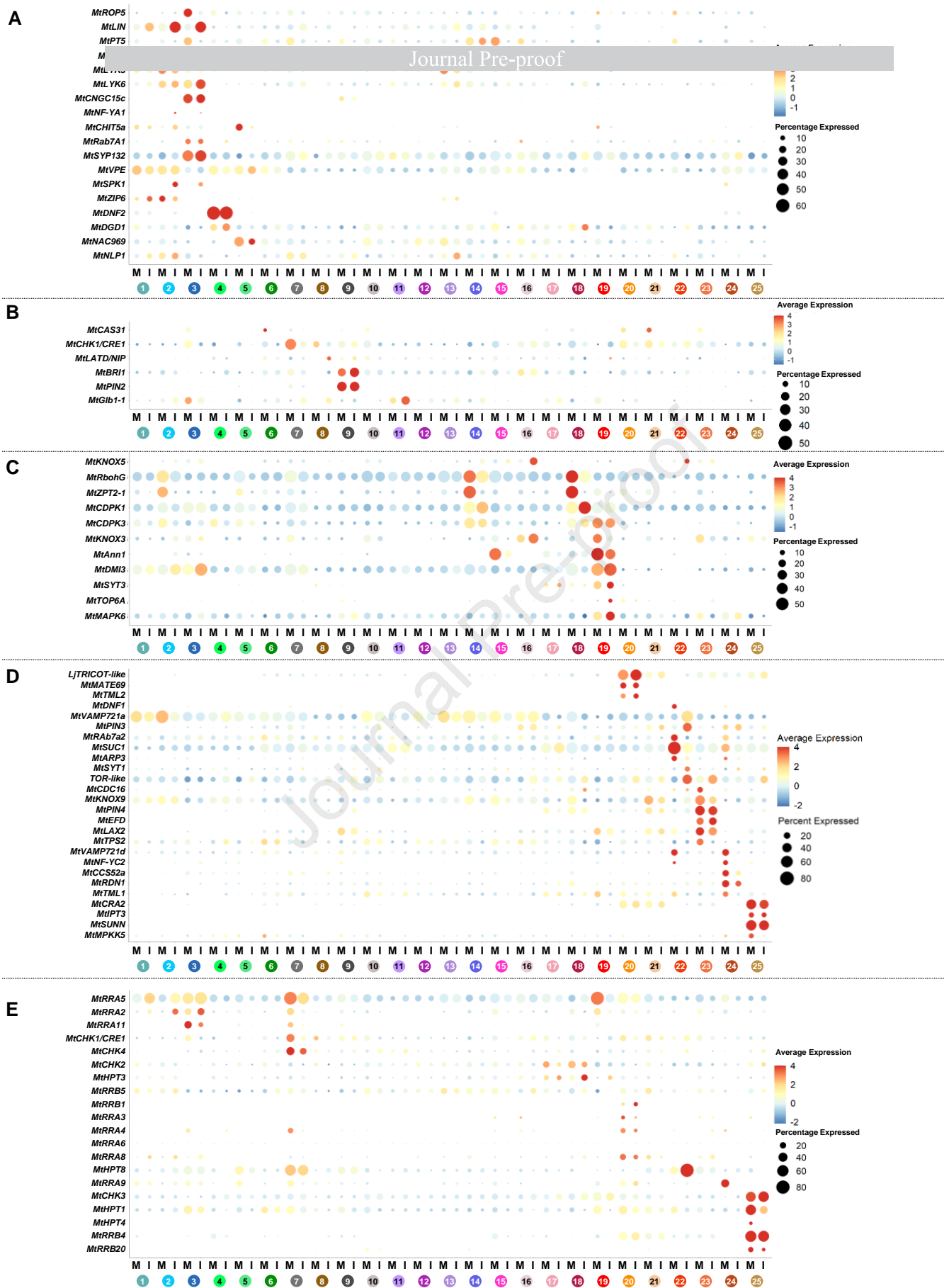


Figure 6.